Atmos. Chem. Phys. Discuss., 15, 15155–15241, 2015
www.atmos-chem-phys-discuss.net/15/15155/2015/
doi:10.5194/acpd-15-15155-2015

Atmospheric Chemistry and Physics Discussions

Evaluating the climate and air quality impacts of short-lived pollutants

A. Stohl[1], B. Aamaas[2], M. Amann[3], L. H. Baker[4], N. Bellouin[4], T. K. Berntsen[2], O. Boucher[5], R. Cherian[6], W. Collins[4,7], N. Daskalakis[8,9], M. Dusinska[1], S. Eckhardt[1], J. S. Fuglestvedt[2], M. Harju[1], C. Heyes[3], Ø. Hodnebrog[2], J. Hao[10], U. Im[8,*], M. Kanakidou[8,9], Z. Klimont[3], K. Kupiainen[3], K. S. Law[11], M. T. Lund[2], R. Maas[12], C. R. MacIntosh[4], G. Myhre[2], S. Myriokefalitakis[8,9], D. Olivié[13], J. Quaas[6], B. Quennehen[11], J.-C. Raut[11], S. T. Rumbold[7], B. H. Samset[2], M. Schulz[13], Ø. Seland[13], K. P. Shine[4], R. B. Skeie[2], S. Wang[10], K. E. Yttri[1], and T. Zhu[14]

[1]NILU – Norwegian Institute for Air Research, Kjeller, Norway
[2]Center for International Climate and Environmental Research – Oslo (CICERO), Oslo, Norway
[3]International Institute for Applied Systems Analysis (IIASA), Laxenburg, Austria
[4]Department of Meteorology, University of Reading, Reading, United Kingdom
[5]LATMOS, Université Pierre et Marie Curie (UPMC)/CNRS, Paris, France
[6]Institute for Meteorology, Universität Leipzig, Germany
[7]Met Office Hadley Centre, Exeter, United Kingdom

[8]Environmental Chemical Processes Laboratory, Department of Chemistry, University of Crete, Heraklion, Crete, Greece
[9]FORTH, ICE-HT, Platani, Patras, Greece
[10]School of Environment, Tsinghua University, Beijing, China
[11]Sorbonne Universités, UPMC Univ. Paris 06, Université Versailles St-Quentin, CNRS/INSU, LATMOS-IPSL, UMR 8190, Paris, France
[12]RIVM – National Institute for Public Health and the Environment, Bilthoven, the Netherlands
[13]Norwegian Meteorological Institute, Oslo, Norway
[14]State Key Laboratory for Environmental Simulation and Pollution Control, College of Environmental Sciences and Engineering, Peking University, Beijing, China
[*]now at: Aarhus University, Department of Environmental Science, Frederiksborgvej 399, 4000 Roskilde, Denmark

Received: 7 May 2015 – Accepted: 12 May 2015 – Published: 3 June 2015

Correspondence to: A. Stohl (ast@nilu.no)

Published by Copernicus Publications on behalf of the European Geosciences Union.

ACPD
15, 15155–15241, 2015

Abstract

This paper presents a summary of the work done within the European Union's Seventh Framework Programme project ECLIPSE (Evaluating the Climate and Air Quality Impacts of Short-Lived Pollutants). ECLIPSE had a unique systematic concept for designing a realistic and effective mitigation scenario for short-lived climate pollutants (SLCPs: methane, aerosols and ozone, and their precursor species) and quantifying its climate and air quality impacts, and this paper presents the results in the context of this overarching strategy. The first step in ECLIPSE was to create a new emission inventory based on current legislation (CLE) for the recent past and until 2050. Substantial progress compared to previous work was made by including previously unaccounted types of sources such as flaring of gas associated with oil production, and wick lamps. These emission data were used for present-day reference simulations with four advanced Earth system models (ESMs) and six chemistry transport models (CTMs). The model simulations were compared with a variety of ground-based and satellite observational data sets from Asia, Europe and the Arctic. It was found that the models still underestimate the measured seasonality of aerosols in the Arctic but to a lesser extent than in previous studies. Problems likely related to the emissions were identified for Northern Russia and India, in particular. To estimate the climate impacts of SLCPs, ECLIPSE followed two paths of research: the first path calculated radiative forcing (RF) values for a large matrix of SLCP species emissions, for different seasons and regions independently. Based on these RF calculations, the Global Temperature change Potential metric for a time horizon of 20 years (GTP_{20}) was calculated for each SLCP emission type. This climate metric was then used in an integrated assessment model to identify all emission mitigation measures with a beneficial air quality and short-term (20 year) climate impact. These measures together defined a SLCP mitigation (MIT) scenario. Compared to CLE, the MIT scenario would reduce global methane (CH_4) and black carbon emissions by about 50 and 80 %, respectively. For CH_4, measures on shale gas production, waste management and coal mines were most important. For

ACPD
15, 15155–15241, 2015

non-CH_4 SLCPs, elimination of high emitting vehicles and wick lamps, as well as reducing emissions from gas flaring, coal and biomass stoves, agricultural waste, solvents and diesel engines were most important. These measures lead to large reductions in calculated surface concentrations of ozone and particulate matter. We estimate that in the EU the loss of statistical life expectancy due to air pollution was 7.5 months in 2010, which will be reduced to 5.2 months by 2030 in the CLE scenario. The MIT scenario would reduce this value by another 0.9 to 4.3 months. Substantially larger reductions due to the mitigation are found for China (1.8 months) and India (11–12 months). The climate metrics cannot fully quantify the climate response. Therefore, a second research path was taken. Transient climate ensemble simulations with these ESMs were run for the CLE and MIT scenarios, to determine the climate impacts of the mitigation. In these simulations, the CLE scenario resulted in a surface temperature increase of 0.70 ± 0.14 K between the years 2006 and 2050. For the decade 2041–2050, the warming was reduced by 0.22 ± 0.07 K in the MIT scenario, and this result was in almost exact agreement with the response calculated based on the emission metrics (reduced warming of 0.22 ± 0.09 K). The metrics calculations suggest that non-CH_4 SLCPs contribute ~ 22 % to this response and CH_4 78 %. This could not be fully confirmed by the transient simulations, which attributed about 90 % of the temperature response to CH_4 reductions. Attribution of the observed temperature response to non-CH_4 SLCP emission reductions and black carbon (BC) specifically is hampered in the transient simulations by small forcing and co-emitted species of the emission basket chosen. Nevertheless, an important conclusion is that our mitigation basket as a whole would lead to clear benefits for both air quality and climate. The climate response from BC reductions in our study is smaller than reported previously, largely because our study is one of the first to use fully coupled climate models, where unforced variability and sea-ice responses may counteract the impacts of small emission reductions. The temperature responses to the mitigation were generally stronger over the continents than over the oceans, and with a warming reduction of 0.44 K (0.39–0.49) largest over the Arctic. Our calculations suggest particularly beneficial climate responses in Southern

ACPD
15, 15155–15241, 2015

Europe, where the surface warming was reduced by about 0.3 K and precipitation rates were increased by about 15 (6–21) mm yr^{-1} (more than 4 % of total precipitation) from spring to autumn. Thus, the mitigation could help to alleviate expected future drought and water shortages in the Mediterranean area. We also report other important results of the ECLIPSE project.

1 Introduction

The United Nations Framework Convention on Climate Change (UNFCCC) requires climate policies to "be cost-effective so as to ensure global benefits at the lowest possible cost" and that "policies and measures should ... be comprehensive ... [and] ... cover all relevant sources, sinks and reservoirs". This was made operational by the Kyoto Protocol, which sets limits on emissions of six different greenhouse gases (GHGs), or groups of GHGs – carbon dioxide (CO_2), methane (CH_4), nitrous oxide (N_2O), perfluorocarbons (PFCs), hydrofluorocarbons (HFCs) and sulfur hexafluoride (SF_6). Collectively these are often known as "the Kyoto gases" or the "Kyoto basket"[1]. CO_2 is the most important anthropogenic driver of global warming, with additional significant contributions from CH_4 and N_2O. However, other anthropogenic emissions capable of causing climate change are not covered by the Kyoto Protocol. Some are covered by other protocols, e.g. emissions of chlorofuorocarbons (CFCs) and hydrochlorofluorocarbons (HCFCs) are regulated by the Montreal Protocol, because of their role in stratospheric ozone (O_3) depletion. But there are others, notably several short-lived

[1]Note that, formally, only species given values of Global Warming Potentials (GWP) in IPCC's Second Assessment Report were controlled during the first commitment period (2008–2012) of the Kyoto Protocol. The second commitment period (2013–2020), via the Doha Amendment, also includes NF_3 in the list of greenhouse gases, and uses GWP values from the IPCC's Fourth Assessment Report. The Doha Amendment is currently not in force, as it awaits ratification by a sufficient number of parties.

ACPD
15, 15155–15241, 2015

components that give strong contributions to climate change that are excluded from existing climate agreements.

In the present study we investigate climate and air quality impacts of the emissions of CH_4, which has a lifetime of about 9 ± 1 years (Prather et al., 2012) and a number of much shorter-lived components (atmospheric lifetimes of months or less) which directly or indirectly (via formation of other short-lived species) influence the climate (Myhre et al., 2013):

- Methane is a greenhouse gas roughly 26 times stronger than CO_2 on a per molecule basis at current concentrations. It is relatively well-mixed in the atmosphere and has both natural and anthropogenic sources. It is also a precursor of O_3 and stratospheric water vapour.
- Black carbon (BC, also commonly known as soot), a product of incomplete combustion of fossil fuels and biomass, affects climate via several mechanisms (Bond et al., 2013). It causes warming through absorption of sunlight and by reducing surface albedo when deposited on snow. BC also affects clouds, with a consequent (but highly uncertain) impact on their distribution and radiative properties (Boucher et al., 2013).
- Tropospheric O_3 is a greenhouse gas produced by chemical reactions from the emissions of the precursors CH_4, carbon monoxide (CO), non-CH_4 volatile organic compounds (NMVOCs) and nitrogen oxides (NO_x). Emissions of these same precursors also impact on hydroxyl radical (OH) concentrations with further impacts especially on CH_4.
- Several components have cooling effects on climate, mainly sulphate aerosol formed from sulphur dioxide (SO_2) and ammonia (NH_3), nitrate aerosol formed from NO_x and NH_3, and organic aerosol (OA) which can be directly emitted or formed from gas-to-particle conversion of NMVOCs. They cause a direct cooling by scattering solar radiation and alter the radiative properties of clouds, very likely leading to further cooling.

ACPD
15, 15155–15241, 2015

We refer to these substances as short-lived climate pollutants (SLCPs) as they also have detrimental impacts on air quality, directly or via formation of secondary pollutants (Kirtman et al., 2013). Notice that we include the precursors of O_3 and secondary aerosols in our definition of SLCPs. We also include CH_4 in our study even though it is included in the Kyoto Protocol, because of its relatively short lifetime compared to that of CO_2 and its importance for air quality via the formation of O_3. We do not include HFCs in our definition of SLCPs, as they have no significant impact on air quality and can be regulated from a climate policy perspective alone. For SLCPs, on the other hand, cost-effective environmental policy measures should be designed such that they optimize both the climate and air quality responses (Schmale et al., 2014). In some instances, control of the emissions of a species is expected to reduce future warming and improve air quality at the same time – a "win-win" situation (Anenberg et al., 2012); in others, the control of emissions may be conflicting, in the sense that it could increase warming while improving air quality (or vice versa) – in this case, emission control involves a "trade-off" between the impacts.

The net climate impact since pre-industrial times of all short-lived components other than CH_4 together is very likely to be cooling due primarily to sulphate aerosols (Myhre et al., 2013). Whilst SLCP reductions are clearly beneficial for air quality, elimination of all current non-CH_4 SLCP emissions would thus very likely lead to extra warming. Nevertheless, targeted emission reductions of selected SLCPs which cause warming (either directly or via formation of secondary species) have the potential to reduce global warming on a short timescale, as well as improving air quality. They may also reduce the rate of warming (Myhre et al., 2011; Shindell et al., 2012) that is important, for example, for the adaptation of ecosystems to climate change (as recognized by UNFCCC Art. 2) and is expected to accelerate in the near future (Smith et al., 2015). Reducing these selected SLCP emissions might be effective to help avoid (or at least delay) certain undesired impacts of climate change (e.g., rapid sea ice loss in the Arctic; Quinn et al., 2008). At least, optimized SLCP emission reductions could help to reduce

ACPD
15, 15155–15241, 2015

the undesired extra climate warming caused by air quality policy measures that often do not consider climate impacts.

There are many studies that explore possibilities and effects of reductions of short-lived components (e.g., Brasseur and Roeckner, 2005; Rypdal et al., 2009a; Kopp and Mauzerall, 2010; Penner et al., 2010; Unger et al., 2010; Shindell et al., 2012; Bond et al., 2013; Bowerman et al., 2013; Rogelj et al., 2014). Given the interest from policymakers in the abatement of SLCPs, an urgent challenge is to determine the exact climate impacts of the different species involved (e.g., Penner et al., 2010). BC has received particular attention as a component for which a specific emission reduction might have an immediate climate benefit (e.g., Bond and Sun, 2005; Boucher and Reddy, 2008; Grieshop et al., 2009; Rypdal et al., 2009b; Berntsen et al., 2010; Bond et al., 2013).

For designing a successful SLCP emission abatement strategy, the key CH_4 sources are relatively straightforward to deal with because their emission profile is dominated by CH_4 (e.g., venting of natural gas, rice paddies, etc.). Combustion sources, however, emit a mix of many different SLCPs (e.g., BC, OA, NO_x, SO_2) as well as CO_2. This makes it difficult to reduce the emissions of warming agents (e.g., BC) alone, as their control often also leads to removal of co-emitted cooling agents (e.g., OA, SO_2). To achieve a climate benefit, abatement strategies will be most effective if they target sources with a high fraction of warming species in their emissions (e.g., diesel vehicles) (Unger et al., 2010).

1.1 Climate effects of SLCPs

There are several distinct issues that have to be addressed in considering the impact of any proposed SLCP abatement strategy. First, there are large uncertainties in estimates of the climate effects of SLCPs (see e.g. Myhre et al., 2013) and thus also in the effects of emission reductions. These apply particularly to the impact of aerosols on cloud properties (e.g. Quaas et al., 2009; Boucher et al., 2013), but there are also difficulties in evaluating direct radiative effects of aerosols.

ACPD
15, 15155–15241, 2015

Second, the climate impact of short-lived components, even when averaged globally, can depend strongly on location and time (e.g., summer vs. winter) of emissions (Fuglestvedt et al., 1999; Wild et al., 2001; Berntsen et al., 2005, 2006; Koch et al., 2007; Naik et al., 2005; Reddy and Boucher, 2007; Shindell and Faluvegi, 2009). For well-mixed gases (e.g. Kyoto gases), a single globally-valid value of Global Warming Potential (GWP – see Sect. 1.2 for more details) can be calculated for a chosen time horizon, and then used to give the so-called "CO_2-equivalent" emissions of a gas. By contrast, for the non-CH_4 SLCPs, the GWP depends significantly on when and where the emission occurs. Not only does this complicate the calculation of GWPs, it also introduces an additional dimension into the framing of climate policy. For instance, the importance of location for BC emissions has received much attention in this context (Ramanathan and Carmichael, 2008; Shindell and Faluvegi, 2009).

Third, inhomogeneity in the climate response to RF is important for SLCPs. The geographical pattern of RF due to the non-CH_4 SLCPs is generally concentrated close to the source of emission, and hence is quite distinct from the global-scale forcing due to the Kyoto gases. The extent to which these heterogeneous forcing patterns will trigger different climate responses compared to well-mixed gases is an unresolved scientific issue, even though the climate response generally occurs on larger spatial scales (but mainly in the hemisphere where the forcing takes place; Joshi et al., 2003; Shindell et al., 2010) than the forcing itself. One example of the issue of inhomogeneity of response concerns the effects of absorption of solar radiation by BC in the Arctic atmosphere. Flanner (2013) has shown that in the Arctic BC located at low altitudes causes a strong local surface warming, but BC located at higher altitudes causes a surface cooling, which is due to the reduced solar radiation reaching the surface. Another important example is emissions of NO_x as these lead to a shorter-lived (and hence more localised) positive RF due to increases in O_3 and a longer-lived (and hence more global) negative RF due to the increased rate of destruction of CH_4. This means that metrics based on global-mean quantities may be poorly representative of the local im-

ACPD
15, 15155–15241, 2015

pacts of an emission as the response depends on both region and timescale (Shine et al., 2005; Lund et al., 2012).

Fourth, SLCPs may have other effects on climate that go beyond global-mean temperature (Andrews et al., 2010; Kvalevåg et al., 2013) such as through changes in the hydrological cycle (Gedney et al., 2014) and in the atmospheric circulation. For example, in South East Europe there are indications that changes in the radiation budget through direct and indirect effects of aerosols have caused circulation, precipitation and evaporation changes (Lelieveld et al., 2002; Tragou and Lascaratos, 2003). Thus, even a cooling component may cause unwanted climate impacts.

Finally, there are important interdependencies between SLCPs and long-term climate change. The climate (and air quality) impacts of SLCPs depend on the atmosphere into which they are emitted – future changes in temperature, humidity, cloud amount, surface albedo, circulation and atmospheric composition are likely to change these impacts (Isaksen et al., 2009). Acting in the other direction, changes in SLCP emissions can impact vegetation via changes in air quality (Sitch et al., 2007; Collins et al., 2010), nutrient deposition (Mahowald, 2011; Wang et al., 2015) or photosynthetic active radiation (Mercado et al., 2009), thereby altering the terrestrial carbon budget and hence future CO_2 concentrations and thus giving the SLCPs a much longer-term impact.

Taking the above points into account, the short lifetimes and regional dependence of the climate impact of SLCP emissions make these species fundamentally different to the long-lived GHGs regulated under the Kyoto Protocol and these impacts and metric values are much more uncertain (Myhre et al., 2013). Furthermore, cooling aerosols may have partly compensated the warming due to well-mixed greenhouse gases in the past, and this masking effect must be considered when determining the sensitivity of the climate system directly from observations (Knutti and Hegerl, 2008; Skeie et al., 2014). This also reduces our ability to calculate future global warming (e.g. Andreae et al., 2005; Meinshausen et al., 2009; Penner et al., 2010). Thus, there is an urgent need to understand and quantify the role that these components may play in interna-

ACPD
15, 15155–15241, 2015

tional efforts to reduce global warming (Jackson, 2009; Berntsen et al., 2010; Arneth et al., 2009; Rypdal et al., 2009b; Molina et al., 2009; Unger et al., 2010).

1.2 Climate metrics to characterise the effect of SLCPs

The Kyoto Protocol to the UNFCCC is a multi-gas climate treaty that required a method to place emissions of different gases on a common scale. It adopted the GWP with a hundred-year time horizon, GWP_{100}, from the IPCC (Intergovernmental Panel on Climate Change) Second Assessment Report as a metric in order to derive so-called CO_2-equivalents for non-CO_2 gas emissions. The GWP has since then been widely used in implementing the Kyoto Protocol, and for other purposes. However, it was not designed with a particular climate policy in mind, and as a result, GWP may not be the best choice for all particular policy objectives (e.g., Tanaka et al., 2009; Fuglestvedt et al., 2010; Myhre et al., 2013; Pierrehumbert, 2014).

The GWP gives the RF due to a pulse emission of a gas or aerosol, integrated over some time horizon, relative to that of CO_2. The choice of time-horizon has a significant impact on the metric value of an emission (e.g. Skodvin and Fuglestvedt, 1997; Shine, 2009; Fuglestvedt et al., 2010; Aamaas et al., 2013) and is a value-laden choice. The time-integrated nature of the GWP means that it retains the memory of short-lived emissions even at long-time horizons, when their forcing and most of the response have subsided.

Several alternatives to the GWP have been proposed and of these, the Global Temperature change Potential (GTP) (Shine et al., 2005, 2007; Fuglestvedt et al., 2010) has attracted most attention (e.g., Reisinger et al., 2010; Boucher and Reddy, 2008; Gillett and Matthews, 2010; Collins et al., 2013). The GTP gives the global-mean surface temperature change some time after a pulse emission, relative to that of CO_2. In contrast to the GWP, it uses temperature as the indicator and is an "end point", rather than an "integrative", metric. Therefore, it does not retain the memory of short-lived emissions in the same way as the GWP. Difficulties with the GTP include its dependence on the

ACPD
15, 15155–15241, 2015

climate sensitivity and on the method of incorporating the ocean's thermal response (Shine et al., 2007; Fuglestvedt et al., 2010; Olivié and Peters, 2013).

The GTP may be more appropriate to target-based climate policies (UNEP/WMO, 2011) where the aim is to keep temperature change below some given limit, such as the 2 °C limit in the UNFCCC's Copenhagen Accord. The choice of time horizon is then no longer so arbitrary, but is linked to the time at which, for example, 2 °C is likely to be reached. This use of the GTP (Shine et al., 2007; Berntsen et al., 2010; Tanaka et al., 2013) mimics the behaviour of more complex (but less transparent) metrics based on integrated assessment models (Manne and Richels, 2001).

In its 5th Assessment Report, the IPCC assessed scientific aspects of climate metrics and their applicability in policy making. It was emphasized that the most appropriate metric and time horizon will depend on which aspects of climate change are considered most important to a particular application. The assessment also pointed out that there are limitations and inconsistencies related to the treatment of indirect effects and feedbacks (e.g., climate-carbon cycle feedbacks) in climate metrics. In this study, we have adopted GTP_{20}, the GTP over a 20 year time horizon, as our key metric, after careful consideration of alternatives (see Sect. 3.4).

1.3 Air quality impacts of SLCPs

The impact of SLCPs on air quality occurs at both the local and regional scale. While local emissions contribute to episodes of high pollution levels which can cause acute health effects, the long-range transport of air pollutants or their precursors even over intercontinental distances (e.g., Stohl and Trickl, 1999; Dentener et al., 2010) can increase the background concentrations upon which pollution episodes are superimposed. This is also important because there is increasing evidence of harmful effects of long-term exposure to particulate matter (PM), O_3, deposited acidifying compounds and nitrogen to human health and vegetation (Anenberg et al., 2012). Thus, the impact of SLCPs on air quality is complex and requires quantification on local to global scales. At international level, these aspects, including emission regulation, are covered

ACPD
15, 15155–15241, 2015

by the UNECE Convention on Long-Range Transboundary Air Pollution (CLRTAP) and its protocols including the Gothenburg Protocol and its amendments.

The International Agency for Research on Cancer classified outdoor air pollution as carcinogenic to humans with sufficient evidence that it causes lung cancer. A positive association with an increased risk of bladder cancer was also demonstrated. It has been estimated that air pollution caused 223 000 deaths from lung cancer worldwide in 2010 (Unger et al., 2010). Air quality guidelines for various substances published by different agencies are listed in Table 1.

Ozone and PM are the most problematic air pollutants with regard to effects on human health (EEA, 2013). Ozone can, through impairment of lung function, lead to premature deaths and increased hospitalization (West et al., 2006). PM was classified as carcinogenic to humans (IARC, 2015; Grosse, 2013). It is estimated, for instance, that an increase of 10 $\mu g\,m^{-3}$ in the concentrations of PM_{10} (PM with diameter smaller than 10 µm) will increase cardiopulmonary mortality by 9 % (Pope et al., 1995). Different aerosol types are considered when assessing climate impacts, whereas air quality legislation is based on the concept of total mass concentrations of particulate matter – either as $PM_{2.5}$ or PM_{10}. It is, however, likely that human health impacts also depend on PM composition. For instance, according to the World Health Organization (WHO), epidemiological evidence indicates an association of daily variation in BC concentrations with short and long term adverse health effects such as all-cause and cardiovascular mortality, and cardiopulmonary hospital admissions. Additionally, BC was classified as possibly carcinogenic to humans (Group 2B) (WHO, 2012). However, concentration-response functions for individual PM components still need to be established. Thus, neither BC nor ultrafine particles are currently covered specifically by EU guidelines (WHO, 2013).

ACPD
15, 15155–15241, 2015

2 Scope and overall concept

The purpose of this paper is to present a summary of the work done within the European Union's Seventh Framework Programme project ECLIPSE (Evaluating the Climate and Air Quality Impacts of Short-Lived Pollutants). ECLIPSE had a unique systematic concept for designing a realistic and effective SLCP mitigation scenario and quantifying its climate and air quality impacts, which is schematically shown in Fig. 1. Other papers describe particular aspects of the ECLIPSE work in more detail, while we here present key ECLIPSE results in the context of this overarching strategy and overall conclusions of the project.

The first step in ECLIPSE was to create a new set of global baseline emissions for the recent past and future (see Sect. 3.1, top of Fig. 1). These emission data were used for present day reference simulations with Earth system models (ESMs) and chemistry transport models (CTMs). The model simulations were compared extensively with a variety of global ground-based and satellite observational data sets, in particular in three target areas (China, Europe and the Arctic, see Sect. 3.2) to evaluate their capabilities to simulate SLCP concentrations.

To study the climate impacts of SLCPs, ECLIPSE followed two paths of research. The first path (the outer part of the spiral in Fig. 1) calculated RF values for a large matrix of SLCP species emissions, for different seasons and regions independently by changing the emissions of one species from one region and one season at a time (see Sect. 3.3). Based on these RF calculations, suitable metrics were chosen to allow the estimation of the climate impact of particular SLCP emissions over different time horizons (see Sect. 3.4).

These metrics were then used to generate an SLCP mitigation scenario to minimize climate impacts that could be contrasted with the current legislation scenario (see the top of Fig. 1). For this, the region-, season- and species-specific matrix of climate impact (as defined by the chosen metric) was used as an input to an integrated assessment model. All region-, season- and sector-specific emission mitigation measures with

ACPD
15, 15155–15241, 2015

a beneficial air quality impact were then evaluated according to their expected climate benefit. Notice here that emission measures typically affect several SLCP species. For every mitigation measure, the emission reduction of every SLCP species was therefore weighted with the chosen climate metric and summed over all emitted SLCP species. Finally, all measures with beneficial air quality and climate impacts were collected in a basket defining the SLCP mitigation scenario (see Sect. 3.5).

The metrics, however, cannot fully quantify the climate response, due to the underlying simplifying assumptions, including linearity, the need to specify particular time horizons and, most importantly, the focus on one single aspect of climate change (global mean temperature for the chosen GTP metric). Therefore, a second research path (the inner part of the spiral in Fig. 1) was taken to determine the climate response for a set of emission reductions for individual SLCP species, using a small ensemble of four advanced Earth system models (ESMs). Furthermore, transient climate ensemble simulations with these ESMs were run for the baseline and emission mitigation scenarios, to calculate the transient climate and air quality impacts of the mitigation scenario (see Sect. 3.6). A comparison between the climate impacts expected from the metrics and those calculated with the transient simulations (left part of the spiral in Fig. 1) closed the loop between the first and the second research path and allowed the evaluation of the consistency of both approaches (see Sect. 3.7).

3 Results

3.1 The ECLIPSE emissions

The ECLIPSE emission data set was created with the GAINS (Greenhouse gas – Air pollution Interactions and Synergies; http://gains.iiasa.ac.at) model (Amann et al., 2011), which provides emissions of long-lived greenhouse gases and shorter-lived species in a consistent framework. The GAINS model holds essential information about key sources of emissions, environmental policies, and mitigation opportunities for about

ACPD
15, 15155–15241, 2015

160 country-regions. The model relies on exogenous projections of energy use, industrial production, and agricultural activity (ECLIPSE scenarios draw on IEA, 2012, for energy and Alexandros and Bruinsma, 2012, for agriculture) for which it distinguishes all key emission sources and control measures. More than 2000 technologies to control air pollutant emissions and at least 500 options to control GHG emissions are included.

Improvements in the emission model were made especially for China (Zhao et al., 2013; Wang et al., 2014), where large changes have occurred recently, but also for Europe where results of the consultation process during the development of scenarios for the review of the EU National Emission Ceilings Directive (Amann and Wagner, 2014) were used. Furthermore, several sources like brick making, oil and gas production, non-ferrous metals and international shipping were reviewed and updated. Finally, a number of previously unaccounted sources were added or specifically distinguished in the model, e.g., wick lamps, diesel generators, and high-emitting vehicles. The global SO_2 inventory used for IPCC's 5th Assessment Report (Klimont et al., 2013) was also developed during ECLIPSE.

All emission data were gridded consistently to a resolution of $0.5^\circ \times 0.5^\circ$ longitude–latitude. The spatial proxies used in GAINS for gridding are consistent with those applied within the IPCC's Representative Concentration Pathways (RCPs) projections as described in Lamarque et al. (2010) and as further developed within the Global Energy Assessment project (GEA, 2012). They were, however, modified to accommodate more recent year-specific information where available, e.g., on population distribution, open biomass burning, location of oil and gas production, and livestock-specific spatial production patterns (Klimont et al., 2013, 2015b). Emissions were also temporally allocated: monthly distribution was provided for all sources and for the residential heating emissions were based on ambient air temperature (see Stohl et al., 2013).

For the first time in a global emission inventory, emissions from flaring of associated gas in oil production were considered directly, including spatial distribution. For BC, these emissions constitute only about 3 % of the global total. However, owing to emissions in Russia, they constitute about one third of all BC emissions north of 60° N and

ACPD
15, 15155–15241, 2015

two thirds of all emissions north of 66° N. Stohl et al. (2013) found that the gas flaring emissions contribute 42 % of all BC found in the Arctic near the surface, and this has improved the performance of the ECLIPSE models in the Arctic.

Figure 2 shows global anthropogenic ECLIPSE emissions for three developed scenarios (Klimont et al., 2015a, b):

- Current legislation (CLE) includes current and planned environmental laws, considering known delays and failures up to now but assuming full enforcement in the future.
- No further control (NFC) uses the same assumptions as CLE until 2015 but no further legislation is introduced subsequently, even if currently committed. This leads to higher emissions than in CLE for most pollutants.
- The ECLIPSE SLCP mitigation scenario (MIT) includes all measures with beneficial air quality and climate impact (according to the climate metric; see Sects. 3.4 and 3.5).

Different versions of the ECLIPSE inventory (available on request from http://eclipse.nilu.no) have been developed and were available at different times for different tasks (Klimont et al., 2015a, b). We describe here the version 5, which was used for the transient climate model simulations (Sect. 3.6). For model evaluation (Sect. 3.2) and climate perturbation simulations in Sect. 3.6, versions 4 and 4a were used which, for the CLE scenario were very similar to version 5 (Klimont et al., 2015a, b).

During the past few decades, there was a strong growth in CO_2 emissions, but the SLCP emissions have followed a different trajectory, at least at the global level. For example, the SO_2 emissions have been decreasing since 1990, with a temporary increase between 2000 and 2005 (Klimont et al., 2013), owing to strong policies and drastic reductions in Europe and North America. The strong development in Asia was offset at the global level by these reductions but in the future, emissions of SO_2 grow again in the CLE scenario, primarily due to a strong increase in India (Klimont et al.,

ACPD
15, 15155–15241, 2015

2013). In fact, also some other SLCPs (e.g., NO_x) show signs of a rebound about the years 2020–2025, when most of the existing policies will have been fully introduced (Klimont et al., 2015a, b). This is driven by increasing fossil fuel use and thus coupled to increasing CO_2 emissions. In the case of BC, GAINS does not predict further growth in emissions, mostly because current policies to reduce coal use in China for cooking and heating seem to be effective and because of the introduced diesel legislation.

The NFC scenario has higher SLCP emissions than the CLE scenario, showing the importance of actual introduction of already planned policies. However, the NFC scenario still might be optimistic as it actually does not assume any failure or further delays in enforcement of pre-2015 laws. The MIT scenario, which shows deep cuts in the emissions of some species, is the result of a climate-optimized SLCP reduction scenario and is described in Sect. 3.5.

Figure 2 indicates a large spread in possible future emission pathways, which for the air pollutants is larger than anticipated in the RCP scenarios, shown by the grey shading. RCP scenarios focused on building future emission scenarios with different radiative forcing (RF) from long-lived GHGs while for air pollutants all assumed a very similar path, strongly linked with the economic growth (Amann et al., 2013). Consequently all air pollutant emissions decline strongly towards 2050 in all RCP scenarios. This is not the case for the ECLIPSE emissions, and the spread is larger than the RCP spread despite the fact that all scenarios follow the same energy use projection.

Emissions from international shipping differ between the ECLIPSE emission versions 4 and 5. Version 4a still drew on the work done for the RCP scenarios, while for the version 5 dataset, the historical emissions rely on the results of Endresen et al. (2007), with activity data projected with growth rates from IEA (2012). This allowed to model region-specific regulation, i.e., specifically in the Emission Control Areas (ECA), and long term targets to reduce the sulphur content of fuels. For aviation, the emissions originate from Lee et al. (2009) and are consistent with the RCP scenarios.

Non-agricultural, open biomass burning emissions are not calculated in the GAINS model and, for the model simulations, were therefore taken from the Global Fire Emis-

ACPD
15, 15155–15241, 2015

sion Database (GFED), version 3.1 (van der Werf et al., 2010) for the years 2008 and 2009 and held constant in simulations of future scenarios. Biogenic emissions originate from the MEGAN database (Guenther et al., 2012; http://lar.wsu.edu/megan/).

3.2 Model evaluation

Using the ECLIPSE version 4a CLE emissions, simulations were carried out with a range of models. In addition to the four ESMs used in ECLIPSE (HadGEM3, ECHAM6-HAM2, NorESM1-M and CESM1/CAM5.2; see Baker et al., 2015a for descriptions of these models), three CTMs and a Lagrangian particle dispersion model were used (see Table 2). All models were run for core periods in 2008 and 2009, when several aircraft campaigns took place in China and the Arctic, but most models simulated the full 2008–2009 period. Some models were also run for longer periods and were evaluated together with other models. For instance, in a comparison against aircraft measurements, Samset et al. (2014) found that the models systematically overpredict BC concentrations in the remote troposphere, especially at higher altitudes. They concluded that the BC lifetime in the models is too long. A follow-up study suggested that the best match to aircraft observations could be achieved with strongly increased BC emissions and decreased lifetimes (Hodnebrog et al., 2014). Daskalakis et al. (2015) derived changes in the local lifetime of BC up to 150 % associated with the use of different amounts and spatial distribution of fire emissions in the same chemistry transport model, demonstrating the dependence of BC lifetime on its emissions. Tsigaridis et al. (2014) found systematic underprediction of OA near the surface as well as a large model divergence in the middle and high troposphere. They attributed these discrepancies to missing or underestimated OA sources, the removal parameterisations as well as uncertainties in the temperature-dependent partitioning of secondary OA in the models. As a consequence of these studies, ECLIPSE models were improved in terms of emissions, secondary OA formation and removal parameterisations.

A detailed evaluation of the performance of the improved ECLIPSE models was made for Eastern Asia, using satellite, airborne and ground-based measurements of

ACPD
15, 15155–15241, 2015

pollutant gases (CO, NO_2, O_3 and SO_2) and aerosols (Quennehen et al., 2015). For Eastern Asia in August–September 2008 (Fig. 3, left two columns), data were averaged over three urban and five rural sites. The models have difficulties reproducing the urban concentrations, due to their coarse resolution. However, surprisingly most models overestimated the urban SO_2 mixing ratios. This could be related to power plant emissions that are actually occurring outside urban boundaries, being placed into the coarse urban model grid cells. For urban NO_2 models deviate less from observations, with both overestimates and underestimates, thus the model mean captures the observations. The measured concentrations of NO_2 and O_3 at the rural sites are matched relatively well (agreement within the range of the temporal distribution at individual sites) but SO_2 is generally overestimated there as well. The most severe problem at rural sites, however, is a systematic underestimation of CO mixing ratios, which was attributed to underestimated CO lifetimes in the models (Quennehen et al., 2015).

A similar comparison was made for Europe with background measurements taken from stations of the European Monitoring and Evaluation Programme (EMEP) (Fig. 3, right two columns for winter and summer). Overall, over Europe the ECLIPSE model mean captures the mean observations with the exception during summer for CO that is underestimated (as in Asia). Summertime O_3 is overestimated by many models at rural locations over Europe and Asia suggesting too much photochemical production downwind of emission regions.

Satellite-derived aerosol optical depth (AOD) measurements were reproduced quite well by the models over China and Europe (Fig. 4). Evaluation of individual aerosol components over Asia (Quennehen et al., 2015) shows an overestimation of the ECLIPSE model-mean surface BC in urban China in summer 2008, which is probably due to the short-term mitigation measures taken during the Olympic Games. Over Europe, ECLIPSE models satisfactorily simulate surface BC observations both in winter and summer (Fig. 4). However, problems were identified over India: Gadhavi et al. (2015) found that BC concentrations are strongly underestimated in Southern India even when aerosol removal processes in one model were completely switched off

ACPD
15, 15155–15241, 2015

in the region. Furthermore, observed AOD values in Northern India are larger than simulated by all but two of the ECLIPSE models (Fig. 4). This suggests that the emissions of BC and precursors of other aerosols are underestimated for India in the ECLIPSE emission data set. This could be related to the rapid recent growth of emissions in India (Klimont et al., 2013), which may be underestimated in the inventories, as well as with problems capturing the true spatial distribution of emissions in India.

The Arctic was shown previously to be a particularly challenging region for aerosol model simulations (e.g., Shindell et al., 2008). An evaluation of the ECLIPSE models over the Arctic was coordinated with the Arctic Monitoring and Assessment Programme (AMAP, 2015). Comparisons were made for BC and sulphate for six ground stations and during six aircraft campaigns (Eckhardt et al., 2015). As an example, a comparison of the BC concentrations simulated by the ECLIPSE models with measured equivalent BC is shown in Fig. 5 for the stations Zeppelin on Svalbard, Pallas in Finland and Tiksi in Siberia. For Zeppelin, most models clearly underestimate the observed concentrations during winter and spring, whereas for Pallas which is closer to source regions, the models tend to overestimate. In general, the model performance (also at other Arctic sites, not shown) is better than in previous comparisons (e.g., Shindell et al., 2008). However, very large model underestimates were found for Tiksi, from where measurement data have only recently become available. Another ECLIPSE study showed that also the snow BC concentrations are generally underestimated by models in Northern Russia but overestimated elsewhere in the Arctic (Jiao et al., 2014). It is therefore likely that the model underestimates are caused by too low BC emissions in Russia in the ECLIPSE CLE data set. Yttri et al. (2014) attribute this at least partly to an underestimation of residential wood burning, based on levoglucosan measurements made at Zeppelin. Eckhardt et al. (2015) suggest that also SO_2 emissions in Northern Russia are underestimated. ECLIPSE models participating in AMAP (2015) also showed a systematic underestimation in CO concentrations in the Arctic and lack of model skill in simulating reactive nitrogen species important for O_3 production.

ACPD
15, 15155–15241, 2015

An important finding of the model-measurement comparisons is that overall the ESMs show a similar performance as the CTMs. This is encouraging for the further use of the ESMs for determining the climate impacts (Sect. 3.6). The comparisons led to some further improvements of the ECLIPSE emissions for version 5, prior to their use for transient climate model simulations. For instance, wick lamps were identified as an important emission source in India, the inclusion of which improved the agreement with the observations in a model sensitivity study (Gadhavi et al., 2015). Other enhancements (e.g., re-gridding of non-ferrous smelter emissions to improve SO_2 emissions in Russia as suggested by Eckhardt et al., 2015) came too late for the climate impact studies and were only made in version 5a.

Another aspect of model evaluation is to determine the capability of models to reproduce past trends, and this was tested over Europe. Strong reductions of aerosol emissions occurred over Europe, since the 1980s due to air quality legislation in Western Europe, and since the early 1990s due to economic restructuring in Eastern Europe. This emission reduction is manifest e.g. in strongly increasing trends in surface solar radiation ("solar brightening") and visibility (Stjern et al., 2011), but also in a stronger warming trend compared to the earlier period in which aerosol emissions increased (Cherian et al., 2014). The "historical" simulations contributed to the 5th Coupled Model Intercomparison Project (CMIP5, Taylor et al., 2012) using previous versions of the ECLIPSE ESMs were assessed for continental Europe, and compared to observations from the Global Energy Balance Archive (Gilgen et al., 1998) and the Climate Research Unit (CRU) of the University of East Anglia (CRU-TS-3.10, Mitchell and Jones, 2005). The 1960–1980 period shows a strong "solar dimming" (reduction in surface solar radiation) and small warming, since the greenhouse-gas-induced warming is offset by the aerosol forcing. The period 1990–2005, in turn, shows the solar brightening, and a much stronger warming. All three tested models are able to reproduce this strong increase in warming trend to within their uncertainties (Fig. 6), suggesting that the climate response to aerosol changes is captured.

ACPD
15, 15155–15241, 2015

3.3 Radiative forcing

To provide input to the metrics needed for designing a mitigation scenario, dedicated model simulations by three ESMs (ECHAM6-HAM2, HadGEM3, NorESM) and a CTM (OsloCTM2) were used to establish a matrix of specific RF (Bellouin et al., 2015) by season and region of emission. Specific RF (SRF) is defined as the RF per unit change in emission rate once the constituents have reached equilibrium and is given in $\mathrm{mW\,m^{-2}\,(Tg\,yr^{-1})^{-1}}$. To estimate SRF, the emissions of eight short-lived species (BC, OA, SO_2, NH_3, NO_x, CO, CH_4 and NMVOCs) were reduced by 20 % compared to their ECLIPSE baseline. These species cause RF themselves and/or lead to the perturbation of radiative forcers (e.g., O_3). The regional reductions were made for Europe and China, as well as for the global shipping sector and for a rest-of-the-world region. To account for seasonal differences in SRF, separate reductions were applied for May–October and November–April. Henceforth we will refer to these as Northern Hemisphere (NH) "summer" and "winter". Notice that in our case the sign of SRF is opposite to that of RF, because the imposed emission changes are negative. A reduction of a warming species gives negative RF values but positive SRF values. It is important to note that SRF excludes rapid adjustments in the atmosphere, with the exception that BC semi-direct effects were calculated explicitly, and stratospheric temperature adjustments were included for O_3 and CH_4.

Models generally agreed on the sign of RF and the ranking of the efficiency of the different emitted species, but disagreed quantitatively (see Bellouin et al., 2015 for details). The best estimate of a species' RF was considered to be the average of all models, with the model spread indicating its uncertainty. However, not all models have calculated RF for all species or have accounted for all processes. For instance, all models were able to quantify the aerosol direct effect but only three quantified the 1st indirect effect. For BC aerosols only one model quantified the snow albedo effect and the semi-direct effect. Therefore, mean RF values were determined by averaging

ACPD
15, 15155–15241, 2015

across all available models for each process separately. In most cases, all four models were available for this, but for some processes fewer models had to be used.

Figure 7 shows the resulting SRF for reductions in the emissions of SO_2, NO_x, CH_4 and BC and the processes contributing to the total forcing, for Europe, China, and on global average. The globally-averaged SRF was obtained by adding RF for Europe, China, and Rest of the World, then normalising to global emission change. The SRF values are largest for BC but note that global emissions of BC are smaller than for the other species. In addition, the semi-direct effect of BC potentially offsets a considerable fraction of the aerosol direct RF and RF due to deposition on snow. Quantifying the semi-direct effect has large uncertainties, however, because internal variability of the climate system masks tropospheric adjustments to BC perturbations. This means that the sign of total SRF exerted by decreases in BC emissions may be negative if a weak BC direct effect is more than compensated by a strong semi-direct effect. Nevertheless, the ECLIPSE BC SRF best estimate of about $50\,mW\,m^{-2}\,(Tg[C]\,yr^{-1})^{-1}$ when semi-direct effects are included is not an outlier compared to previous estimates, which range from 24 to $108\,mW\,m^{-2}\,(Tg[C]\,yr^{-1})^{-1}$ according to Table 23 of Bond et al. (2013). Moreover, ECLIPSE simulations indicate that the magnitude of the semi-direct effect is smaller than the direct aerosol effect (Hodnebrog et al., 2014; Samset and Myhre, 2015), in agreement with most, but not all, previous studies (again, see Table 23 of Bond et al., 2013). Reductions in the emissions of light scattering aerosols such as sulphate stemming from its precursor SO_2 induce a negative SRF. The RF values of aerosols are generally larger for summer emissions than for winter emissions because of the stronger insolation. However, there are exceptions to this. For instance, the BC deposition on snow is more effective for winter emissions because of the larger snow extent in winter and spring and partial preservation of deposited BC into spring. Aerosol SRF is also larger in magnitude for Europe than for China, most likely because of different cloud regimes which are differently affected by semi-direct and indirect aerosol effects.

ACPD
15, 15155–15241, 2015

For NO_x, SRF is uncertain because decreases in NO_x emissions perturb tropospheric chemistry in two opposite ways, working on different timescales: first, they reduce tropospheric O_3 concentrations, thus exerting a positive SRF. Second, they increase CH_4 concentrations, thus exerting a negative SRF, with an additional CH_4-induced change in O_3. ECLIPSE accounts for those two pathways, and quantifies a third, whereby reductions in NO_x emissions suppress nitrate aerosol formation and its associated RF. ECLIPSE is therefore able to state with confidence that NO_x exerts a negative SRF, because the O_3 response is not sufficient to offset the combined CH_4 and nitrate response. For CH_4, ECLIPSE finds a relatively large range of SRF estimates from the models. This range does not reflect uncertainties in the absorbing properties of CH_4. Rather, the range reflects the different CH_4 lifetimes in the models – and the changes in these lifetimes – and hence the sensitivities of the burdens to emission changes.

3.4 Climate metrics

ECLIPSE explored various options for climate metrics. In addition to selecting the most useful metric for designing the mitigation scenario, the project also made conceptual developments. Collins et al. (2013) developed further the application of Regional Temperature change Potential (RTP) presented by Shindell et al. (2012) by accounting for the location of emissions, thereby opening for regionality for both drivers and responses. Collins et al. (2013) also expanded the GTP concept by tentatively including the climate-carbon feedback for the non-CO_2 gases. So far, this feedback has only been included for the reference gas CO_2 which means that GTPs (and GWPs) tend to underestimate the relative effect of non-CO_2 components (Myhre et al., 2013). Furthermore, Shine et al. (2015) present a new metric named the Global Precipitation change Potential (GPP), which is designed to gauge the effect of emissions on the global water cycle. Of particular relevance for SLCPs is their demonstration of a strong near-term effect of CH_4 on precipitation change and the role of sustained emissions of BC and sulphate in suppressing precipitation.

ACPD
15, 15155–15241, 2015

Aamaas et al. (2013) investigated several different metrics and showed that emissions of CO_2 are important regardless of what metric and time horizon is used, but that the importance of SLCP varies greatly depending on the metric choices made. MacIntosh et al. (2015) considered the errors made when calculating RF and climate metrics from multi-model ensembles in different ways. They showed that the mean metric values are relatively robust but the estimation of uncertainties is very dependent on the methodology adopted. Finally, Lund et al. (2014a) applied climate metrics to quantify the climate impacts of BC and co-emitted SLCPs from on-road diesel vehicles, and Lund et al. (2014b) considered the special case of a fuel switch from diesel to biodiesel.

As explained in Sect. 3.5, climate metrics were used in ECLIPSE to identify specific sets of air pollution reduction measures that result in net positive climate effects (i.e., reduced warming), considering the impacts on all co-controlled substances. Based on the RF results shown in Sect. 3.3, Aamaas et al. (2015) calculated regional and seasonal GTP and GWP metrics for the SLCP emissions, for various time horizons, and explored their properties. Of all the explored metrics, the pollution control analysis was carried out for GWP_{100} and GTP_{20}, as these two metrics showed large differences in their quantifications. It was found, however, that the emerging basket of emission control measures was very similar for both, although the ranking of the potential climate impacts of individual measures was sometimes different, with larger effect of CH_4-related measures for the GWP_{100} metric (due to the higher value this metric with longer time horizon assigns to CH_4).

In the following, we concentrate our analysis on the GTP_{20} metric, which is shown in Fig. 8 for a pulse emission relative to an equal mass emission of CO_2 for a selected number of species. The metric builds on and reflects important aspects of the RF forcing values shown in Fig. 7. For example, for most species GTP_{20} values for summer are larger than values for winter (see, e.g., results for SO_2), and values for Europe are larger than values for Asia. While SO_2 only has negative values (i.e., reduction of SO_2 always leads to warming), the opposite is true for CH_4. Figure 8 also shows the contribution from different processes to the total GTP_{20} metric, and for BC and NO_x they

ACPD
15, 15155–15241, 2015

are often of different sign and their magnitude strongly depends on the emission region and season. While all of this was accounted for in GAINS (see Sect. 3.5), it is clear that this makes the choice of mitigation options more uncertain, and this is further complicated by the fact that BC and NO_x emissions are always associated with co-emissions of other SLCPs (e.g., OA). The GTP_{20} metric was determined also for all other SLCPs (not shown).

For the implementation of mitigation measures, a pulse emission metric is not very realistic, as measures are normally introduced gradually, become more effective with time, and are usually maintained indefinitely. Therefore, we also considered versions of the GTP and GWP metrics for sustained emission measures and a linear ramp-up of emission measures over a 15 year time period (Aamaas et al., 2015; see also Boucher and Reddy, 2008). We chose the ramp-up version of the GTP_{20} metric for designing our mitigation scenario with the GAINS model (see Sect. 3.5), as it most realistically reflects the implementation of mitigation measures. Notice that the ramp-up version of the GTP_{20} metric can be derived directly from its pulse emission version, by linear combination of emission pulses (see Aamaas et al., 2015, for details). Figure 8 shows the pulse emission version because pulse emissions are building blocks for various versions of the metrics, including the ramp-up version.

To go beyond global mean temperature, it is also possible to calculate regional surface temperature changes using the regional temperature potentials (RTP) concept of Shindell and Faluvegi (2009). This concept maps RF in one given latitude band to the temperature response in several other latitude bands and was adopted by us (Aamaas et al., paper in preparation). For the mapping, we used the pre-calculated RTP-coefficients of Shindell and Faluvegi (2009). Even though the coefficients are likely model-dependent, we had to use these values because they are not available from any other model (and specifically not from the ECLIPSE models). We made two additions, however, for BC in the Arctic and BC on snow using the method of Lund et al. (2014a) with results from Samset et al. (2013) and Flanner (2013). Using the RTP concept and RF calculations from Sect. 3.3 (Bellouin et al., 2015), we calculated absolute regional

ACPD
15, 15155–15241, 2015

temperature change potentials (ARTP) for the set of components, regions and seasons for which ECLIPSE has determined RF values (Fig. 7). Following Collins et al. (2013), the ARTPs were used to estimate transient surface warming using an impulse response function for temperature response from Boucher and Reddy (2008) (as was also used for the GTP calculations). Details of the method and ARTP values will be given in Aamaas et al. (paper in preparation) and results of the ARTP calculations will be used in Sect. 3.7 for comparisons with transient ESM runs.

3.5 Emission mitigation and air quality impacts

For designing a climate-optimized SLCP emission mitigation scenario, the CO_2-equivalent SLCP emissions were minimized using the GAINS model. For this, the numerical values of the GTP_{20} metric for the final year 2035 for each species, region and season were implemented into GAINS. The ramp-up version of this metric assumes a linear implementation of mitigation measures between the years 2015 and 2030 and thereafter a full implementation. Mitigation measures typically affect several species at the same time. For instance, controlling BC emissions leads to a "co-control" of OA and other species. The GTP_{20} metric values are different for all of these species and can be of different sign, and it is important to determine the net impact of a mitigation measure across all affected species. In practice, the species-specific metric values were weighted with the emission factors to obtain the net metric value for each of the $\sim$ 2000 mitigation measures in every one of the 168 regions considered in GAINS, and for summer and winter periods separately. These measures were subsequently ranked according to their CO_2-equivalent total net climate impact as measured by the GTP_{20} metric, and all measures with a beneficial climate and air quality impact were included in the mitigation (MIT) scenario basket (Klimont et al., 2015b); this approach is consistent with that taken by UNEP/WMO (2011) and Shindell et al. (2012).

The mitigation basket contains three groups of measures: (1) measures that affect emissions of CH_4 that can typically be centrally implemented (e.g., by large energy companies, municipalities, etc.) and which also impact background O_3, (2) technical

ACPD
15, 15155–15241, 2015

measures that reduce the emissions of BC, mainly for small stationary and mobile sources, (3) non-technical measures to eliminate BC emissions, e.g., through economic and technical assistance to the poorest population. While about 220 GAINS model measures were collected in the mitigation basket, they were merged into representative measure groups. For example, high emitters are calculated for each of the GAINS transport subsectors and fuels while here removing high emitters is represented by one "measure". Similarly for cooking stoves, GAINS estimates mitigation potential for various types of fuels but all of these are included further into one category "clean cooking stoves". Also for CH_4, losses from gas distribution are calculated for several GAINS end use sectors while here the mitigation potential is reported under one measure where leaks from low pressure pipelines are reduced. Finally, for NMVOCs all of the solvent related options in GAINS (over 50) are categorized as one measure reducing losses from solvent use activities. Considering the above, about 50 "measures" represent the about 220 GAINS options that were included in the mitigation basket. The 17 most effective measures contribute 80 % of the total climate benefit, according to the GTP_{20} metric, with CH_4 measures contributing about 47 % and BC-focused measures contributing 33 %. These measures are listed in Table 3. It is interesting to notice that the top CH_4 and BC-focused measures both concern the oil and gas industry and specifically the venting or flaring of associated gas.

As can be seen in Fig. 2, the mitigation has only minor effects on CO_2 emissions, but reduces most SLCPs strongly compared to the CLE scenario. By 2030, CH_4 emissions are reduced by about 50 % and BC emissions by nearly 80 %. OA is co-controlled with BC, causing a nearly 70 % (not shown) reduction of its emissions, as for some sectors BC outweighs the cooling effects of OA. While NO_x emission reductions are in most cases also not preferred by the GTP_{20} metric (see Fig. 8), reductions stem from the co-control when higher Euro standards are introduced; they reduce significantly several pollutants such as BC, CO, NMVOC and also NO_x (Klimont et al., 2015a, b). By contrast, SO_2 emissions are nearly the same in both the CLE and MIT scenarios, as for the key sectors emitting SO_2, the warming by SO_2 reductions (see Fig. 8) cannot

ACPD
15, 15155–15241, 2015

be outweighed by co-control of species whose reduction would lead to cooling. Thus, SO_2 reductions are largely avoided.

The global CO_2-equivalent emissions (calculated using the GTP_{20} metric values) are shown as a function of time in Fig. 9. Values are shown for CLE and MIT and are split into contributions from CH_4 and other SLCP emissions. For comparison, CO_2 emissions are also shown. On the short time scale of the GTP_{20} metric, CH_4 and CO_2 emissions are nearly equally important in the CLE scenario. The CO_2-equivalent emissions of CH_4 are, however, reduced by 50 % in MIT. The CO_2-equivalent emissions for the other SLCPs are negative in both scenarios, indicating that in total they have a cooling impact. As the mitigation reduces preferentially warming components, this cooling becomes even stronger in the MIT case. The total CO_2-equivalent emissions (including CO_2 emissions) are reduced substantially in the MIT scenario (blue shaded area in Fig. 9 shows the reduction), for example by about 70 % in the year 2030. About 56 % of this reduction is due to CH_4 measures and ~ 44 % is due to other measures. It is important to notice that the effect of the SLCP mitigation is relatively large for the rather short time horizon of the GTP_{20} metric; it would be smaller for a longer time horizon. Similarly, the relative importance of CH_4 compared to other SLCP emissions would be increased for a longer time horizon.

Surface concentrations of SLCPs resulting from the CLE and MIT scenarios were determined from the various model simulations. Figure 10 shows maps of the model-mean relative differences for O_3 and $PM_{2.5}$ for the last decade (2041–2050) of the transient simulations and Table 4 reports differences for several regions shown with boxes in Fig. 10. Concentrations of O_3 (Fig. 10, upper panel) are reduced globally, with reductions of more than 12 % in most of the Northern Hemisphere and the strongest reductions of up to about 20 % occurring in East Asia. For instance, in Eastern China (see Table 4), O_3 is reduced by 19.3 % (16.0–24.4 %). BC and OA concentrations (not shown) were also globally reduced, with BC reductions reaching more than 80 %. For sulphate (not shown), the relative changes are much smaller than for BC and OA and both increases and decreases occur – a consequence of the relatively small global

ACPD
15, 15155–15241, 2015

SO_2 emission reductions (see Fig. 2). Changes in $PM_{2.5}$ concentrations (Fig. 10, lower panel) are smaller because of large contributions from natural sources (e.g., sea salt, dust, wildfire emissions). $PM_{2.5}$ concentrations in the SLCP source regions were reduced by typically 10–20 % and up to nearly 50 % in smaller regions. Reductions are strongest in Asia, for instance 19.8 % (17.9–22.5 %) in India (Table 4).

In summary, air pollutant concentrations in the MIT scenario are dramatically reduced compared to the CLE scenario, especially in the polluted (and heavily populated) source regions. This indicates the beneficial effect of the SLCP mitigation on air quality. Nevertheless, a word of caution is needed for O_3. The O_3 concentrations increase strongly (typically between 5 and 20 %, depending on region and season) between now and 2050 in the CLE scenario, because of increasing CH_4 and NO_x emissions. Therefore, global mean O_3 concentrations even in the MIT scenario do not decrease substantially with time. However, strong relative O_3 reductions by the mitigation are simulated in the SLCP source regions (Table 4), which more than outweigh the overall concentration increase in the CLE scenario. Therefore, population exposure to O_3 decreases with time in the MIT scenario.

For Europe and Asia, the GAINS model also contains source-receptor relationships which allow the estimation of the impacts of emissions on human health. GAINS quantifies the impacts of changes in SLCP emissions on the long-term population exposure to $PM_{2.5}$ in Europe, China and India and estimates the resulting premature mortality, in terms of reduced statistical life expectancy and cases of premature deaths (Amann et al., 2011). Calculations follow the recommendations of the findings of the WHO review on health impacts of air pollution and recent analyses conducted for the Global Burden of Disease project (Lim et al., 2012), relying on the results of the American Cancer Society cohort study (Pope et al., 2002) and its re-analysis (Pope et al., 2009). It uses cohort- and country-specific mortality data extracted from life table statistics to calculate for each cohort the baseline survival function over time.

Using GAINS, we estimate that in the EU the loss of statistical life expectancy will be reduced from 7.5 months in 2010 to 5.2 months in 2030 in the CLE scenario. The

ACPD
15, 15155–15241, 2015

ECLIPSE mitigation measures (MIT) would reduce statistical life shortening by another 0.9 months (Fig. 11, upper panel), resulting in 4.3 months of reduction in life expectancy. This value is only slightly above the target of 4.1 months that has been set by the European Commission in its 2013 Clean Air Policy proposal (EC 2013). Population in non-EU countries would gain approximately one month life expectancy from the implementation of the ECLIPSE measures in 2030 (Fig. 11, upper panel).

In China and India, the potential health gains from the implementation of the ECLIPSE measures are significantly larger, however, starting from a substantially higher level of life shortening due to $PM_{2.5}$ (Fig. 11, lower panel). In China, the ECLIPSE measures would in the year 2030 extend the life expectancy of the population by approximately 1.8 months and reduce the premature deaths attributable to $PM_{2.5}$ by 150 000–200 000 cases year^{-1}.

In India, rapid increase in energy consumption, together with lacking regulations on emission controls for important sources (e.g., power generation) and poor enforcement of existing laws (e.g., for vehicle pollution controls) will lead to a steep increase in $PM_{2.5}$ levels. If no saturation of health impacts is assumed for such high levels (there are no cohort studies available for such high concentrations), with conservative assumptions GAINS estimates approximately 850 000 cases annually of premature deaths from air pollution in 2010. For 2030, $PM_{2.5}$ exposure would increase by more than 50 %, and at the same time the population would increase and age. Combined, these factors would let the premature deaths from air pollution grow by approximately 125 % to 1.9 million cases in 2030, with another doubling to 3.7 million cases in 2050. Against this background, the ECLIPSE measures would avoid more than 400 000 cases of premature deaths in 2030 and almost 700 000 in 2050. Using the loss in statistical life expectancy as an alternative metric, the ECLIPSE measures would gain 11–12 months to the Indian population (Fig. 11, lower panel).

ACPD
15, 15155–15241, 2015

3.6 Climate impacts

The climate impacts of SLCPs were determined with four ESMs (HadGEM3, NorESM, ECHAM6-HAM2/MPIOM, and CESM-CAM4) in two different experiments. In the first experiment, still part of the outer loop of the spiral in Fig. 1, all land-based anthropogenic emissions of each of SO_2, OA and BC were removed one at a time and the models were run to equilibrium; in the other experiment, the mitigation scenario described in Sect. 3.5 was followed in a series of transient ensemble model runs, constituting the inner spiral loop in Fig. 1.

For the first experiment, described in Baker et al. (2015a), the four ESMs, with full ocean coupling were run for a control simulation and a perturbation run for 50 years, after a spin-up period to equilibrium. The control simulation used ECLIPSE V4a emissions for the year 2008 (except for CESM-CAM4, which used year 2000 emissions). For the perturbation, 100 % of the land-based emissions of the three individual species were removed in turn to achieve discernible climate responses. While only three ESMs ran the experiments for SO_2 and OA, all four ESMs ran the BC experiment and two of these used two ensemble members each. Only NorESM included the effect of albedo reduction by BC deposited on snow and ice.

When removing SO_2 emissions, all three models show an increase of global mean surface temperature (Fig. 12a) by 0.69 K (0.40–0.84 K) on average. Here, the first value is the multi-model mean, whereas the values in brackets give the full range of results obtained with the individual models. We will keep this notation throughout the rest of the paper, unless otherwise noted. The zonal mean temperature change is positive at all latitudes and increases with latitude in the Northern Hemisphere, reaching 2.46 K (1.38–3.31 K) at the North Pole (Fig. 13a). It is also positive for most regions of the Earth and is more positive over the continents than over the oceans (Baker et al., 2015a). The models also agree that removing SO_2 emissions results in an increase in global mean precipitation (Fig. 12b), which is in line with the expected impact from a global temperature increase. The precipitation increases are particularly strong over

ACPD
15, 15155–15241, 2015

India and China because of a northward shift of the Intertropical Convergence Zone (ITCZ, see Fig. 13b), which is in accordance with previous studies (e.g. Broccoli et al., 2006).

The response to removing anthropogenic BC emissions, −0.05 K (−0.15 to +0.08 K), is much smaller than the SO_2 response and the models do not all agree on the sign of the global mean response. The multi-model mean is slightly negative (Fig. 12a) but within ±0.5 K everywhere on the globe (not shown) and the zonal mean temperature response differs from model to model (Fig. 13c). The NorESM model shows the strongest cooling in the Arctic, likely because it is the only model accounting for snow albedo changes. Precipitation changes from removing BC emissions are also small, but consistently positive in all models (Fig. 12b) despite the cooling in most models. This is consistent with calculations of the relationship between atmospheric RF and precipitation change in Andrews et al. (2010) and Kvalevåg et al. (2013) (see also Shine et al., 2015). The multi-model temperature response to removing OA emissions is similar to that for removing SO_2, but much weaker overall (Figs. 12a and 13e).

In summary, the emission perturbation studies show that elimination of anthropogenic SO_2 emissions leads to robust warming, elimination of OA also leads to – albeit much weaker – warming, whereas elimination of BC leads to a small temperature response with substantial differences between the models but slight cooling in the multi-model mean. This could be due to the different sizes of the indirect and semi-direct effects of BC in different models, shown in ECLIPSE (Hodnebrog et al., 2014), and possibly to unforced responses of climate system components, especially sea ice, that happen to counteract the small temperature response.

The second ESM experiment simulated the transient responses to the climate-optimized SLCP mitigation of Sect. 3.5 (Baker et al., 2015b). For this, the four ESMs ran three ensemble members each for both the CLE and MIT scenario until the year 2050. The CLE scenario resulted in an increase of global mean surface temperature of 0.70±0.14 K (the value following the "±" sign gives the standard deviation obtained from all ensemble members) between the years 2006 and 2050 in the multi-model ensemble

ACPD
15, 15155–15241, 2015

mean. A large part of this increase is a response to increasing CO_2 concentrations, and consequently the MIT scenario also showed an (albeit smaller) temperature increase. As we here are mainly interested in the response to the SLCP mitigation, we only consider the difference between the MIT and the CLE scenario in the following. Time series of the global mean temperature difference between the two scenarios are shown in Fig. 14. There is a considerable spread between individual ensemble members even from the same model. This reflects simulated natural climate variability superimposed on the response to the SLCP mitigation, which makes diagnosis of the latter difficult. Systematically negative global mean temperature responses emerge only when the mitigation measures are fully implemented. The multi-model mean global temperature (MIT-CLE) difference is -0.22 ± 0.07 K for the final 10 years, confirming that the mitigation could be successful in reducing the warming of the CLE scenario.

The relative cooling is particularly strong over the continents and weakest over the Northern North Atlantic (not shown), similar to the response patterns seen in the perturbation simulations. Figure 15 shows mean temperature responses for the last decade of the simulation, for various regions. The strongest relative cooling between MIT and CLE of about 0.44 K (0.39–0.49 K) are found for the Arctic, with peak values of about 0.62 K (0.37–0.84 K) occurring in autumn (winter values are similar). Over Europe, differences are more consistent between models and more strongly negative in the southern parts than in the northern parts (see also Fig. 16). This can be explained by the larger natural climate variability in Northern Europe. Mainly small and inconsistent results are found over India, due to model differences in the shift of the ITCZ, whereas changes over China and North America are consistently negative from (almost) all models and for all seasons.

The precipitation responses are less robust which, in the tropics, is due to model differences in the migration of the ITCZ. Nevertheless, there are regions with consistent responses of all models. Of particular interest is the precipitation increase over Southern Europe (Fig. 16). Seen against the background of expected warming and drying in the Mediterranean area due to CO_2-driven climate change, the precipitation

ACPD
15, 15155–15241, 2015

increase due to the SLCP mitigation would be beneficial, especially given the fact that it is strongest from spring to autumn (Fig. 17), with 15 (6–21) mm yr^{-1} increase (corresponding to more than 4 % (2–6 %) of total precipitation) and combined with a temperature reduction that is also largest during that period (Fig. 15). Thus, our mitigation approach would help to alleviate drought and water shortages in the Mediterranean area in summer, as they are expected for the future (Orlowsky and Seneviratne, 2012).

In the aerosol perturbation experiments, we have seen that SO_2 emission reductions lead to strong warming and OA reductions to weaker warming, whereas BC emission reductions lead to much weaker and model-dependent cooling. While the GTP_{20} metric attributes ∼ 44 % of the reduction in CO_2-equivalent emissions to BC-related measures, it was interesting to clarify whether this is reflected in the transient climate model simulations, and how this fraction changes with time. For this, two additional experiments with four ensemble members each were run with one ESM (CESM-CAM4) with a slab ocean representation (for greater computational efficiency): one with all emission reductions (MIT), and one with only CH_4 emission reductions (MIT-CH_4-only). Ozone reductions resulting from CH_4 emission measures are included in the MIT-CH_4-only simulations, whereas O_3 changes from non-CH_4 measures are omitted. The two experiments yielded a relatively similar temporal characteristic of global mean temperature difference (see Fig. 18), where the MIT scenario led to 0.45 ± 0.04 K less warming than CLE, and the MIT-CH_4-only scenario led to 0.41 ± 0.04 K less warming than CLE for the final decade of the simulation (2041–2050). The difference between the two scenarios is not significant, owing to the small number of ensemble members. Thus, the simulations indicate a dominant (∼ 90 %) role of CH_4 emission reductions and a small (∼ 10 %) but perhaps non-negligible role of non-CH_4 mitigation measures for reducing the warming by 2041–2050.

Notice that the warming reduction for the MIT scenario with the slab-ocean version of the CESM-CAM4 model is twice as strong as with the more realistic full-ocean version shown in Fig. 14. However, given the results with the slab-ocean version, a dominant role of CH_4 in the mitigation is likely also for the full-ocean simulations. In fact, this

ACPD
15, 15155–15241, 2015

adds to the explanation why the temperature response in Fig. 14 emerges from natural variability only about 10 years (i.e., approximately the lifetime of CH_4) after the start of the mitigation measures.

We have seen in Sect. 3.5 that the chosen set of mitigation measures also leads to considerable reductions in PM and O_3 and thus improves air quality. If implemented as such, the mitigation package as a whole would therefore have beneficial impacts on both air quality and climate. However, the experiments conducted here also suggest that the co-benefits for climate and air quality result mainly from CH_4 mitigation, which improves air quality (via clear reductions of the background surface O_3 concentrations) and reduces warming considerably. The co-benefits of the non-CH_4 SLCP mitigation measures, on the other hand, are quite limited. These measures improve air quality strongly (via reductions of PM concentrations and O_3) but reduce warming only slightly. This does of course not mean that all of the individual measures have small co-benefits. For instance, it is likely that mitigating sources with the highest BC/OA ratio would lead to larger co-benefits. Partly, the small co-benefits for the non-CH_4 SLCP measures are a result of the design of our MIT scenario, which was based on the GTP_{20} metric and this seems to suggest a stronger warming reduction due to non-CH_4 SLCP measures than seen in the transient ESM simulation results. The consistency between the two approaches will be discussed in the next section, but it is clear that if the metric was too "optimistic" with respect to the achievable warming reductions by non-CH_4 SLCP mitigation measures, some individual measures will have been included in the MIT basket, which in the transient simulations might have actually led to warming enhancement instead of warming reduction.

3.7 Closing the loop: climate impacts from metric calculations and transient model simulations, and applications of the metrics

The purpose of this section is to compare the climate impacts of the SLCP mitigation as estimated with the metrics and as obtained from the transient simulations, as well as to show applications of the metrics. A perfect agreement between the two meth-

ACPD
15, 15155–15241, 2015

ods cannot be expected, as the metrics assume linearity of the climate response to all individual forcing contributions and are also valid for a specific time horizon. Furthermore, after using the RF values calculated in ECLIPSE, the methodology adopted to calculate the GTP values uses a representation of both the size and time dependence of the response derived from one particular (pre-ECLIPSE) ESM calculation. Since the different ESMs used in ECLIPSE have a diverse range of climate sensitivities and different representations of uptake of heat by the oceans, this is a further important reason why exact agreement should not be expected. The metrics are also calculated for a specific climate and are less accurate for periods with a changed climate. One example is the BC snow albedo effect, which is gradually reduced over time because the snow and ice extent decreases as the climate warms. On the other hand, diagnosis of temperature responses from the transient climate simulations is also associated with large error bars because of natural climate variability. Nevertheless, a comparison of the two methods is an important consistency check but, to our knowledge, has never been done before for a SLCP mitigation scenario and using an ensemble of ESMs.

The ARTP metric described in Sect. 3.5, applied over a series of timescales, allows calculation of the regional (in broad latitude bands) temperature response from the reduction of individual species in the mitigation basket as a function of time. Based on these regional responses a total global mean response is derived which can be compared directly with the global mean temperature difference between the MIT and CLE transient simulations in the ESMs.

The ARTPs depend on the global climate sensitivity assumed for the impulse response function used (Shindell et al., 2012). To provide a consistent comparison with the ESM transient simulations, the ARTPs have been scaled by the individual climate sensitivities for each ESM. Furthermore, not all the ESMs include all components and forcing mechanisms in their transient simulations, e.g., only NorESM includes the forcing due to BC deposited on snow and ice. To make a consistent comparison, ARTP contributions were summed only over the components and processes included in each ESM. Figure 19 shows the global mean temperature responses using the ARTP

ACPD
15, 15155–15241, 2015

method, which can be compared directly with the temperature changes obtained by the transient ESM simulations shown in Fig. 14. The solid lines in Fig. 19 show the total global temperature response of the mitigation, while the dashed lines show the contribution from CH_4 reductions only. For the last decade of the simulation (2041–2050) both the ESMs and ARTPs give a mean global response of −0.22 K. The ranges of the estimates based on the four models are also very similar (−0.15 to −0.29 K for the ESMs, and −0.13 to −0.33 K for the ARTPs). Note, however, that the factors contributing to these ranges are not the same in these two estimates. For the ESMs, the differences in radiative forcing, the models' climate sensitivities and internal variability determine the range, while for the ARTP-based estimate the differences in which processes causing RF are included in each model and the model's climate sensitivites are accounted for. The ranking of the responses between the individual models are, however, not identical. Nevertheless, based on these results we conclude that for the global mean response to SLCP mitigation the ARTP-based method simulates well the full ESM simulations to estimate the impact of SLCP mitigation.

The ARTP-based method suggests a larger contribution of non-CH_4 SLCPs to the temperature response for the 2041–2050 decade (∼ 22 %, see dashed lines in Fig. 19) than the transient simulations using the slab-ocean version of the CESM-CAM4 model discussed in the previous section (∼ 10 %). One reason for this disagreement is that many of the BC-related measures included in the mitigation basket were relatively OC-rich and this makes their net temperature response extremely uncertain, especially when aerosol indirect effects and the semi-direct effect are considered. An even larger contribution (44 %) of non-CH_4 SLCPs to the CO_2-equivalent emission reductions of the MIT scenario was obtained with the GTP_{20} metric directly (see Sect. 3.5). However, this value is valid only for the temperature response in the year 2035, for which the relative contribution of the non-CH_4 SLCPs (which are shorter-lived than CH_4) is larger than for later years. As the diagnostic uncertainties for a single year are very large for the transient ESM simulations, we abstain from comparisons. Direct comparisons

ACPD
15, 15155–15241, 2015

are anyway not meaningful, since the metrics include all recognized RF mechanisms, whereas most ESMs lack some of these (e.g., snow albedo changes by BC).

To further investigate the ability of a simplified metrics method to represent the regional response simulated by the ESMs, we use the ARTPs to estimate the response in four broad latitude bands and these results can be compared to the corresponding results from the ESMs. Figure 20 shows the 20 year mean results (2031–2050) for both methods. The general pattern of the responses with largest impact for the main source region at Northern Hemisphere Mid-Latitudes (NHML) and in the Arctic is well captured by the ARTP method. However, as expected the agreement between the estimates is not as good as for the global mean (correlation coefficient of 0.68 for the 16 data points). The ARTP-based estimates are close to the ESM means for the NHML and the Tropics, while for the Arctic and for the SH the ARTP method underestimates the response simulated by the ESMs. The reason for the more pronounced Arctic amplification in our ESMs than for the ARTPs is probably a less pronounced Arctic amplification in the model of Shindell and Faluvegi (2009), from where the RTP-coefficients were taken. For future development and use of the ARTP method, RTP-coefficients are needed also from other ESMs.

The motivation for establishing these ARTPs is that after quality-control they provide policy-makers with a relatively simple tool to quantify how sectorial emissions (i.e., by region, sector and component) contribute to temperature change over time in broad latitude bands. Figure 21 illustrates this potential for the MIT scenario. It shows the responses (mean of the ARTP-based estimates for the four ESMs) for mitigation taking place in Europe, China and globally. The larger relative impact on the Arctic by mitigation of European emissions compared to mitigation in China is clearly seen, while the impact for NHML is about three times larger in absolute terms for mitigation of SLCPs in China. These results can then easily be further analysed by separating the impact by emitted species (Fig. 21d), or by separating the impact of a single emission sector. Figure 22, for instance, shows the estimated impact on Arctic temperatures by global mitigation of SLCPs from the residential heating and cooking sector, broken down to

ACPD
15, 15155–15241, 2015

contributions from individual SLCP species. Notice that it would be prohibitively expensive to run an ensemble of ESM simulations that is large enough to detect the small temperature response resulting from such minute emission changes.

4 Conclusions

ECLIPSE has come to a number of important scientific conclusions, which are also of high relevance for climate and air quality policy:

- ECLIPSE has created a new inventory for anthropogenic SLCP emissions, including scenarios for the future. An important finding is the large range of possible future developments of anthropogenic SLCP emissions, which even for a single future energy pathway substantially exceeds the range of SLCP emissions given in IPCC's RCPs. The large range results from the uncertainties of future air quality policies, as well as from the expected level of implementation and enforcement of existing policies (Klimont et al., 2015a, b).

- Detailed comparisons between measured and modelled distributions of aerosol, O_3 and other SLCP gases have shown that for many substances the models are in good agreement with available background observations. The model performance of the ESMs is similar to that of CTMs. For BC, in particular, the agreement between models and measurements has improved for the Arctic (Eckhardt et al., 2015), which is partly the result of accounting for emissions from gas flaring and emission seasonality (Stohl et al., 2013). Outside the Arctic, a reduction of the BC lifetime led to improvements (Samset et al., 2014). Nevertheless, our comparisons suggest underestimates of BC and aerosol precursor emissions in high-latitude Russia and in India. Furthermore, it was found that SO_2 concentrations are overestimated and CO concentrations are underestimated by the models (Quennehen et al., 2015) at the surface in Asia and Europe during summer and autumn. The CO underestimate is likely associated with a too short CO lifetime in the mod-

ACPD
15, 15155–15241, 2015

els. Ozone, on the other hand, is generally overestimated at rural locations. Such discrepancies may affect model responses to emission perturbations and thus radiative forcing.

- Earth System Models can reproduce the accelerated upward trend of surface temperature over Europe that was observed when aerosol precursor emissions were reduced in the 1990s (leading to solar brightening), after a period of emission growth in the 1960s–1980s (leading to solar dimming) (Cherian et al., 2014).

- ECLIPSE performed detailed multi-model calculations of RF for all considered SLCP species, as a function of emission region and season. It is found that the absolute values of specific RF for aerosols are generally larger in summer than in winter (Bellouin et al., 2015). It is found that the semi-direct effect on clouds, although highly uncertain, can potentially offset a considerable fraction of the direct positive RF of BC. This, together with reduced BC lifetimes, causes the net RF for BC calculated in ECLIPSE to be only weakly positive, which is different from most previous studies.

- NO_x emissions affect the concentrations of O_3, CH_4 and nitrate aerosols. The first effect leads to positive RF, while the latter two cause negative RF. We have quantified all these effects and can state with confidence that the current net RF of global historical NO_x emissions is negative. The forward looking metrics GWP and GTP for NO_x are negative as well, except for short time horizons.

- ECLIPSE had a focus on calculation and testing of emission metrics, which led to a better understanding of existing metrics (Aamaas et al., 2013), further development of the applications of the RTP concept (Collins et al., 2013) and introduction of new metric concepts such as the Global Precipitation change Potential (GPP) by Shine et al. (2015). After careful consideration of the alternatives, we chose a 15 year ramp-up version (i.e., assuming a linear implementation of measures) of the GTP_{20} metric for designing a SLCP mitigation scenario.

ACPD
15, 15155–15241, 2015

– The GTP_{20} metric was implemented into the GAINS model to identify mitigation measures (MIT) that have beneficial impacts on both air quality and climate. We find that the 17 most important mitigation measures would contribute more than 80 % of the climate benefits according to the GTP_{20} metric. The top measures both for CH_4 and BC mitigation are to prevent the venting (for CH_4) and flaring (for BC) of gas associated with the oil production. For CH_4, measures on shale gas production, waste management and coal mines were also important. For non-CH_4 SLCPs, elimination of high emitting vehicles and wick lamps, as well as reducing emissions from coal and biomass stoves, agricultural waste, solvents and diesel engines were also important.

– Full implementation of these measures (the MIT scenario) would reduce global anthropogenic emissions of CH_4 and BC by 50 and 80 %, respectively. As a result of co-control with BC, emissions of organic aerosols would also be reduced by 70 %, whereas emissions of CO_2 and SO_2 would hardly be changed. Based on the GTP_{20} metric, the CO_2-equivalent emissions (including CO_2 emissions) would be decreased by about 70 % in the year 2030, with about 56 % of the decrease caused by CH_4 measures and 44 % caused by non-CH_4 SLCP measures.

– The mitigation scenario would reduce surface concentrations of O_3 and $PM_{2.5}$ globally compared to the CLE scenario, with BC reductions of more than 80 % in some areas. We estimate that in the EU the loss of statistical life expectancy due to air pollution will be reduced from 7.5 months in 2010 to 5.2 months in 2030 in the CLE scenario. The MIT measures would gain another 0.9 months. Substantially larger health improvements from SLCP measures are estimated for China (1.8 months) and India (11–12 months).

– Climate impacts of SLCP emissions were simulated with four ESMs with full ocean coupling. Equilibrium simulations that removed all land-based anthropogenic emissions of SO_2, BC and OA in turn showed robust global-mean increase in surface temperatures of 0.69 K (0.40–0.84 K) for SO_2 removal and smaller warm-

ACPD
15, 15155–15241, 2015

ing for OA removal (Baker et al., 2015a). The global mean temperature response to BC removal was slightly negative: −0.05 K (−0.15 to 0.08 K). The relatively small global response to BC emission reductions was attributed to strong, while uncertain, indirect and semi-direct effects, which partly offset the direct aerosol radiative effect.

– Climate impacts of the MIT scenario were investigated with ESM ensemble transient simulations of both the CLE and MIT scenario (Baker et al., 2015b). Multi-model ensemble mean global mean surface temperature in the CLE scenario increased by 0.70 ± 0.14 K between the years 2006 and 2050. The ensemble mean global mean surface warming for the last decade of the simulation (2041–2050) was, however, 0.22 ± 0.07 K weaker for the MIT scenario, demonstrating the effect of the SLCP mitigation. The response was strongest in the Arctic, with warming reduced by about 0.44 K (0.39–0.49 K).

– In addition to global annual mean temperature change, there are other climate parameters that are of relevance for policy decisions (e.g., changes in precipitation, regional temperatures, etc.). The SCLP reductions in the MIT scenario led to particularly beneficial climate responses in Southern Europe, where the surface warming was reduced by about 0.3 K from spring to autumn and precipitation rates were increased by about 15 (6–21) mm yr^{-1} (15 mm yr^{-1} corresponding to more than 4 % of total precipitation), compared to the CLE scenario. Thus, the mitigation could help to alleviate expected future drought and water shortages in the Mediterranean region.

– Additional ESM transient simulations, which only included the CH_4 emission reductions, led to a global warming reduction that amounted to about 90 % of the reduction produced by the simulations using the full set of measures for the final decade of the simulations (2041–2050). This suggests that, for longer time horizons, the net climate benefits from our chosen non-CH_4 SLCP mitigation measures in terms of global annual mean temperature change are limited, probably

ACPD
15, 15155–15241, 2015

due to small forcing and co-emitted cooling species. Nevertheless, if implemented as such, the mitigation package as a whole would have beneficial impacts on both air quality and climate, and for the latter, also in other climate variables than global annual mean temperature change such as regional changes in temperature and precipitation.

– For the first time, ECLIPSE compared the temperature response to an SLCP mitigation scenario as it is given by climate metrics (using the ARTP method) and as it is simulated with transient ESM simulations. This is crucial for the application of metrics, which – because of their simplicity and flexibility – are very relevant in a policy context where they can substitute full ESM simulations which are expensive and impractical for small perturbations. Both approaches give a global mean reduced warming of the surface temperatures by 0.22 K (and similar uncertainty ranges) for the period 2041–2050. Also the large-scale pattern of the response (with strongest warming reductions in the Arctic) is reproduced similarly by both methods, even though the agreement is less good than for the global mean.

– The metrics-based approach and the transient model simulations agree less well on the relative contribution of CH_4 and non-CH_4 SLCP mitigation measures to the reduced warming. While the metrics-based approach suggests that the non-CH_4 measures account for 22 % of the global-mean temperature response for 2041–2050, the transient simulations result in a contribution from non-CH_4 measures of only about 10 %. One reason for this disagreement is that many of the BC-related measures included in the mitigation basket were relatively OC-rich and this makes their net temperature response more uncertain, especially when aerosol indirect effects are considered. Furthermore, small cooling influences are easily masked by unforced variability in fully-coupled climate simulations.

– The major share of the cooling effect in our SLCP mitigation scenario is contributed by CH_4 reductions, with 20–30 % of the difference in near-term global mean climate warming from the reduction of non-CH_4 SLCPs (multi-model range

ACPD
15, 15155–15241, 2015

0.01–0.06 K for time periods from 2021–2040, according to metrics-based estimates). Thus, to maximize climate co-benefits of non-CH_4 SLCPs, sources with the highest BC/OA emission ratios should be addressed with priority. At the same time, air pollution policies should consider mitigation of CH_4, with clear co-benefits for climate warming and air quality via reduced surface O_3 concentrations.

Acknowledgements. The research leading to these results has received funding from the European Union Seventh Framework Programme (FP7/2007-2013) under grant agreement no 282688 – ECLIPSE.

References

Aamaas, B., Peters, G. P., and Fuglestvedt, J. S.: Simple emission metrics for climate impacts, Earth Syst. Dynam., 4, 145–170, doi:10.5194/esd-4-145-2013, 2013.

Aamaas, B., Berntsen, T. K., Fuglestvedt, J. S., Shine, K. P., and Bellouin, N.: Multimodel emission metrics for regional emissions of short lived climate forcers, Atmos. Chem. Phys., in preparation, 2015.

Alexandratos, N. and Bruinsma, J.: World agriculture towards 2030/2050, the 2012 revision (No. 12-03), ESA Working Paper, World Food and Agricultural Organization, Rome, Italy, 2012.

Amann, M. and Wagner, F.: A Flexibility Mechanism for Complying with National Emission Ceilings for Air Pollutants, TSAP Report #15, Version 1.0, International Institute for Applied Systems Analysis IIASA, Laxenburg, Austria, 2014.

Amann, M., Bertok, I., Borken-Kleefeld, J., Cofala, J., Heyes, C., Höglund-Isaksson, L., Klimont, Z., Nguyen, B., Posch, M., Rafaj, P., Sandler, R., Schöpp, W., Wagner, F., and Winiwarter, W.: Cost-effective control of air quality and greenhouse gases in Europe: modeling and policy applications, Environ. Modell. Softw., 26, 1489–1501, doi:10.1016/j.envsoft.2011.07.012, 2011.

Amann, M., Klimont, Z., and Wagner, F.: Regional and global emissions of air pollutants: recent trends and future scenarios, Annu. Rev. Env. Resour., 38, 31–55, 2013.

AMAP: AMAP Assessment 2015: Black Carbon and Ozone as Arctic Climate Forcers. Arctic Monitoring and Assessment Programme (AMAP), Oslo, Norway, in preparation, 2015.

ACPD
15, 15155–15241, 2015

Andreae, M. O., Jones, C. D., and Cox, P. M.: Strong present-day aerosol cooling implies a hot future, Nature, 435, 1187–1190, 2005.
Andrews, T., Forster, P. M., Boucher, O., Bellouin, N., and Jones, A.: Precipitation, radiative forcing and global temperature change, Geophys. Res. Lett., 37, L14701, doi:10.1029/2010GL043991, 2010.
Anenberg, S. C., Schwartz, J., Shindell, D., Amann, M., Faluvegi, G., Klimont, Z., Janssens-Maenhout, G., Pozzoli, L., van Dingenen, R., Vignati, E., Emberson, L., Muller, N. Z., West, J. J., Williams, M., Demkine, V., Hicks, W. K., Kuylenstierna, J., Raes, F., and Ramanathan, V.: Global air quality and health co-benefits of mitigating near-term climate change through methane and black carbon emission controls, Environ. Health Persp., 120, 831–839, doi:10.1289/ehp.1104301, 2012.
Arneth, A., Unger, N., Kulmala, M., and Andreae, M. O.: Clean the air, heat the planet?, Science, 326, 672–673,doi:10.1126/science.1181568, 2009.
Baker, L. H., Collins, W. J., Olivié, D. J. L., Cherian, R., Hodnebrog, Ø., Myhre, G., Quaas, J., and Samset, B. H.: Climate responses to anthropogenic emissions of short-lived climate pollutants, Atmos. Chem. Phys. Discuss., 15, 3823–3862, doi:10.5194/acpd-15-3823-2015, 2015a.
Baker, L. H., Collins, W., Cherian, R., Quaas, J., Olivie, D., Hodnebrog, O., and Myhre, G.: Transient simulations of the ECLIPSE mitigation scenario, in preparation, 2015b.
Bellouin, N., Baker, L., Hodnebrog, Ø., Oliviè, D., Cherian, R., Barber, C., Samset, B., Esteve, A., Aamaas, B., Quaas, J., and Myhre, G.: Regional and seasonal radiative forcing by perturbations to aerosol and ozone precursor emissions, Atmos. Chem. Phys., in preparation, 2015.
Bentsen, M., Bethke, I., Debernard, J. B., Iversen, T., Kirkevåg, A., Seland, Ø., Drange, H., Roelandt, C., Seierstad, I. A., Hoose, C., and Kristjánsson, J. E.: The Norwegian Earth System Model, NorESM1-M – Part 1: Description and basic evaluation of the physical climate, Geosci. Model Dev., 6, 687–720, doi:10.5194/gmd-6-687-2013, 2013.
Berntsen, T. K., Fuglestvedt, J. S., Joshi, M. M., Shine, K. P., Stuber, N., Ponater, M., Sausen, R., Hauglustaine, D. A., and Li, L.: Climate response to regional emissions of ozone precursors: sensitivities and warming potentials, Tellus B, 57, 283–304, 2005.
Berntsen, T. K., Fuglestvedt, J., Myhre, G., Stordal, F., and Berglen, T. F.: Abatement of greenhouse gases: does location matter?, Climatic Change, 74, 377–411, 2006.

ACPD
15, 15155–15241, 2015

Berntsen, T. K., Tanaka, K., and Fuglestvedt, J. S.: Does black carbon abatement hinder CO_2 abatement? A letter, Climatic Change, 103, 627–633, doi:10.1007/s10584-010-9941-3, 2010.

Bond, T. C. and Sun, H. L.: Can reducing black carbon emissions counteract global warming?, Environ. Sci. Technol., 39, 5921–5926, 2005.

Bond, T. C., Doherty, S. J., Fahey, D. W., Forster, P. M., Berntsen, T., DeAngelo, B. J., Flanner, M. G., Ghan, S., Kärcher, B., Koch, D., Kinne, S., Kondo, Y., Quinn, P. K., Sarofim, M. C., Schultz, M. G., Schulz, M., Venkataraman, C., Zhang, H., Zhang, S., Bellouin, N., Guttikunda, S. K., Hopke, P. K., Jacobson, M. Z., Kaiser, J. W., Klimont, Z., Lohmann, U., Schwarz, J. P., Shindell, D., Storelvmo, T., Warren, S. G., and Zender, C. S.: Bounding the role of black carbon in the climate system: a scientific assessment, J. Geophys. Res., 118, 5380–5552, doi:10.1002/jgrd.50171, 2013.

Boucher, O. and Reddy, M. S.: Climate trade-off between black carbon and carbon dioxide emissions, Energy Policy, 36, 193–200, 2008 (see corrigendum on http://www.lmd.jussieu.fr/~obolmd/PDF/Corrigendum_Boucher_Reddy_Energy_Policy_2008.pdf).

Boucher, O., Randall, D., Artaxo, P., Bretherton, C., Feingold, G., Forster, P., Kerminen, V.-M., Kondo, Y., Liao, H., Lohmann, U., Rasch, P., Satheesh, S. K., Sherwood, S., Stevens, B., and Zhang, X. Y.: Clouds and aerosols, in: Climate Change 2013: the Physical Science Basis. Contribution of Working Group I to the Fifth Assessment Report of the Intergovernmental Panel on Climate Change, edited by: Stocker, T. F., Qin, D., Plattner, G.-K., Tignor, M., Allen, S. K., Boschung, J., Nauels, A., Xia, Y., Bex, V., and Midgley, P. M., Cambridge University Press, Cambridge, UK and New York, NY, USA, 571–657, 2013.

Bowerman, N. H. A., Frame, D. J., Huntingford, C., Lowe, J. A., Smith, S. M., and Allen, M. R.: The role of short-lived climate pollutants in meeting temperature goals, Nature Climate Change, 3, 1021–1024, doi:10.1038/nclimate2034, 2013.

Brasseur, G. P. and Roeckner, E.: Impact of improved air quality on the future evolution of climate, Geophys. Res. Lett., 32, L23704, doi:10.1029/2005GL023902, 2005.

Broccoli, A. J., Dahl, K. A., and Stouffer, R. J.: Response of the ITCZ to Northern Hemisphere cooling, Geophys. Res. Lett., 33, L01702, doi:10.1029/2005GL024546, 2006.

Cherian, R., Quaas, J., Salzmann, M., and Wild, M.: Pollution trends over Europe constrain global aerosol forcing as simulated by climate models, Geophys. Res. Lett., 41, 2176–2181, doi:10.1002/2013GL058715, 2014.

ACPD
15, 15155–15241, 2015

Collins, W. J., Sitch, S., and Boucher, O.: How vegetation impacts affect climate metrics for ozone precursors, J. Geophys. Res., 115, D23308, doi:10.1029/2010JD014187, 2010.
Collins, W. J., Fry, M. M., Yu, H., Fuglestvedt, J. S., Shindell, D. T., and West, J. J.: Global and regional temperature-change potentials for near-term climate forcers, Atmos. Chem. Phys., 13, 2471–2485, doi:10.5194/acp-13-2471-2013, 2013.
Daskalakis, N., Myriokefalitakis, S., and Kanakidou, M.: Sensitivity of tropospheric loads and lifetimes of short lived pollutants to fire emissions, Atmos. Chem. Phys., 15, 3543–3563, doi:10.5194/acp-15-3543-2015, 2015.
Dentener, F., Keating, T., and Akimoto, H. (Eds.): Hemispheric Transport of Air Pollution 2010 – Part A: Ozone and Particulate Matter, Air Pollution Studies No. 17, United Nations, New York, Geneva, 2010.
EC: Proposal for a Directive of the European Parliament and of the Council on the reduction of national emissions of certain atmospheric pollutants and amending Directive 2003/35/EC, European Commission (EC), Brussels, Belgium, 2013.
Eckhardt, S., Quennehen, B., Olivié, D. J. L., Berntsen, T. K., Cherian, R., Christensen, J. H., Collins, W., Crepinsek, S., Daskalakis, N., Flanner, M., Herber, A., Heyes, C., Hodnebrog, Ø., Huang, L., Kanakidou, M., Klimont, Z., Langner, J., Law, K. S., Massling, A., Myriokefalitakis, S., Nielsen, I. E., Nøjgaard, J. K., Quaas, J., Quinn, P. K., Raut, J.-C., Rumbold, S. T., Schulz, M., Skeie, R. B., Skov, H., Lund, M. T., Uttal, T., von Salzen, K., Mahmood, R., and Stohl, A.: Current model capabilities for simulating black carbon and sulfate concentrations in the Arctic atmosphere: a multi-model evaluation using a comprehensive measurement data set, Atmos. Chem. Phys. Discuss., 15, 10425–10477, doi:10.5194/acpd-15-10425-2015, 2015.
EEA: Air quality in Europe – 2013 report, EEA report 9/2013, ISBN 978-92-9213-406-8, available at: http://www.eea.europa.eu/publications/air-quality-in-europe-2013, (last access: 28 April 2014), 2013.
Endresen, Ø., Sørgård, E., Behrens, H. L., Brett, P. O., and Isaksen, I. S. A.: A historical reconstruction of ships' fuel consumption and emissions, J. Geophys. Res., 112, D12301, doi:10.1029/2006JD007630, 2007.
Flanner, M. G.: Arctic climate sensitivity to local black carbon, J. Geophys. Res.-Atmos., 118, 1840–1851, doi:10.1002/jgrd.50176, 2013.

ACPD
15, 15155–15241, 2015

Fuglestvedt, J. S., Berntsen, T. K., Isaksen, I. S. A., Mao, H. T., Liang, X. Z., and Wang, W. C.: Climatic forcing of nitrogen oxides through changes in tropospheric ozone and methane; global 3D model studies, Atmos. Environ., 33, 961–977, 1999.

Fuglestvedt, J. S., Shine, K. P., Berntsen, T., Cook, J., Lee, D. S., Stenke, A., Skeie, R. B., Velders, G. J. M., and Waitz, I. A.: Transport impacts on atmosphere and climate: metrics, Atmos. Environ., 44, 4648–4677, doi:10.1016/j.atmosenv.2009.04.044, 2010.

Gadhavi, H. S., Renuka, K., Ravi Kiran, V., Jayaraman, A., Stohl, A., Klimont, Z., and Beig, G.: Evaluation of black carbon emission inventories using a Lagrangian dispersion model – a case study over southern India, Atmos. Chem. Phys., 15, 1447–1461, doi:10.5194/acp-15-1447-2015, 2015.

GEA: Global Energy Assessment: Toward a Sustainable Future, Cambridge University Press, Cambridge, United Kingdom, 2012.

Gedney, N., Huntingford, C., Weedon, G. P., Bellouin, N., Boucher, O., and Cox, P. M.: Detection of solar dimming and brightening effects on Northern Hemisphere river flow, Nat. Geosci., 7, 796–800, doi:10.1038/ngeo2263, 2014.

Gent, P. R., Danabasoglu, G., Donner, L. J., Holland, M. M., Hunke, E. C., Jayne, S. R., Lawrence, D. M., Neale, R. B., Rasch, P. J., Vertenstein, M., Worley, P. H., Yang, Z.-L., and Zhang, M.: The Community Climate System Model version 4, J. Climate, 24, 4973–4991, doi:10.1175/2011jcli4083.1, 2011.

Gilgen, H., Wild, M., and Ohmura, A.: Means and trends of shortwave irradiance at the surface estimated from global energy balance archive data, J. Climate, 11, 2042–2061, 1998.

Gillett, N. P. and Matthews, H. D.: Accounting for carbon cycle feedbacks in a comparison of the global warming effects of greenhouse gases, Environ. Res. Lett., 5, 034011, doi:10.1088/1748-9326/5/3/034011, 2010.

Grell, G. A., Peckham, S. E., Schmitz, R., McKeen, S. A., Frost, G., Skamarock, W. C., and Eder, B.: Fully coupled online chemistry within the WRF model, Atmos. Environ., 39, 6957–6975, 2005.

Grieshop, A. P., Reynolds, C. C. O., Kandlikar, M., and Dowlatabadi, H.: A black-carbon mitigation wedge, Nat. Geosci., 2, 533–534, 2009.

Grosse, L. Y., Lauby-Secretan, B., El Ghissassi, F., Bouvard, V., Benbrahim-Tallaa, L., Guha, N., Baan, R., Mattock, H., and Straif, K.: The carcinogenicity of outdoor air pollution, Lancet, 14, 1262–1263, 2013.

ACPD
15, 15155–15241, 2015

Guenther, A. B., Jiang, X., Heald, C. L., Sakulyanontvittaya, T., Duhl, T., Emmons, L. K., and Wang, X.: The Model of Emissions of Gases and Aerosols from Nature version 2.1 (MEGAN2.1): an extended and updated framework for modeling biogenic emissions, Geosci. Model Dev., 5, 1471–1492, doi:10.5194/gmd-5-1471-2012, 2012.

Hewitt, H. T., Copsey, D., Culverwell, I. D., Harris, C. M., Hill, R. S. R., Keen, A. B., McLaren, A. J., and Hunke, E. C.: Design and implementation of the infrastructure of HadGEM3: the next-generation Met Office climate modelling system, Geosci. Model Dev., 4, 223–253, doi:10.5194/gmd-4-223-2011, 2011.

Hodnebrog, Ø., Myhre, G., and Samset, B.: How shorter black carbon lifetime alters its climate effect, Nature Communications, 5, 5065, doi:10.1038/ncomms6065, 2014.

IARC: IARC Monographs on the Evaluation of Carcinogenic Risks to Humans, Vol. 109, Outdoor Air Pollution, International Agency for Research on Cancer, Lyon, in press, 2015.

IEA (International Energy Agency): Energy Technology Perspectives. 2012 – Pathways to a Clean Energy System, OECD/IEA, Paris, 2012.

Im, U., Christodoulaki, S., Violaki, K., Zampas, P., Kocak, M.,Daskalakis, N., Mihalopoulos, N., and Kanakidou, M.: Atmospheric deposition of nitrogen and sulfur over southern Europe with focus on the Mediterranean and the Black Sea, Atmos. Environ., 81, 660–670, doi:10.1016/j.atmosenv.2013.09.048, 2013.

Isaksen, I. S. A., Granier, C., Myhre, G., Berntsen, T. K., Dalsøren, S. B., Gauss, M., Klimont, Z., Benestad, R., Bousquet, P., Collins, W., Cox, T., Eyring, V., Fowler, D., Fuzzi, S., Jöckel, P., Laj, P., Lohmann, U., Maione, M., Monks, P., Prevot, A. S. H., Raes, F., Richter, A., Rognerud, B., Schulz, M., Shindell, D., Stevenson, D. S., Storelvmo, T., Wang, W.-C., van Weele, M., Wild, M., and Wuebbles, D.: Atmospheric composition change: climate-chemistry interactions, Atmos. Environ., 43, 5138–5192, 2009.

Jackson, S. C.: Parallel pursuit of near-term and long-term climate mitigation, Science, 326, 526–527, 2009.

Jiao, C., Flanner, M. G., Balkanski, Y., Bauer, S. E., Bellouin, N., Berntsen, T. K., Bian, H., Carslaw, K. S., Chin, M., De Luca, N., Diehl, T., Ghan, S. J., Iversen, T., Kirkevåg, A., Koch, D., Liu, X., Mann, G. W., Penner, J. E., Pitari, G., Schulz, M., Seland, Ø., Skeie, R. B., Steenrod, S. D., Stier, P., Takemura, T., Tsigaridis, K., van Noije, T., Yun, Y., and Zhang, K.: An AeroCom assessment of black carbon in Arctic snow and sea ice, Atmos. Chem. Phys., 14, 2399–2417, doi:10.5194/acp-14-2399-2014, 2014.

ACPD
15, 15155–15241, 2015

Joshi, M., Shine, K., Ponater, M., Stuber, N., Sausen, R., and Li, L.: A comparison of climate response to different radiative forcings in three general circulation models: towards an improved metric of climate change, Clim. Dynam., 20, 843–854, 2003.

Kanakidou, M., Duce, R. A., Prospero, J. M., Baker, A. R., Benitez-Nelson, C., Dentener, F. J., Hunter, K. A., Liss, P. S., Mahowald, N., Okin, G. S., Sarin, M., Tsigaridis, K., Uematsu, M., Zamora, L. M., and Zhu, T.: Atmospheric fluxes of organic N and P to the global ocean, Global Biogeochem. Cy., 26, GB3026, doi:10.1029/2011gb004277, 2012.

Kawamoto, T., Pham, T. T., Matsuda, T., Oyama, T., Tanaka, M., Yu, H. S., and Uchiyama, I.: Historical review on development of environmental quality standards and guideline values for air pollutants in Japan, Int. J. Hyg. Envir. Heal., 214, 296–304, doi:10.1016/j.ijheh.2011.05.007, 2011.

Kirkevåg, A., Iversen, T., Seland, Ø., Hoose, C., Kristjánsson, J. E., Struthers, H., Ekman, A. M. L., Ghan, S., Griesfeller, J., Nilsson, E. D., and Schulz, M.: Aerosol–climate interactions in the Norwegian Earth System Model – NorESM1-M, Geosci. Model Dev., 6, 207–244, doi:10.5194/gmd-6-207-2013, 2013.

Kirtman, B., Power, S. B., Adedoyin, J. A., Boer, G. J., Bojariu, R., Camilloni, I., Doblas-Reyes, F. J., Fiore, A. M., Kimoto, M., Meehl, G. A., Prather, M., Sarr, A., Schär, C., Sutton, R., van Oldenborgh, G. J., Vecchi, G., and Wang, H. J.: Near-term climate change: projections and predictability, in: Climate Change 2013: the Physical Science Basis. Contribution of Working Group I to the Fifth Assessment Report of the Intergovernmental Panel on Climate Change, edited by: Stocker, T. F., Qin, D., Plattner, G.-K., Tignor, M., Allen, S. K., Boschung, J., Nauels, A., Xia, Y., Bex, V., and Midgley, P. M., Cambridge University Press, Cambridge, UK, and New York, NY, USA, 953–1028, 2013.

Klimont, Z., Smith, S. J., and Cofala, J.: The last decade of global anthropogenic sulfur dioxide: 2000–2011 emissions, Environ. Res. Lett., 8, 014003, doi:10.1088/1748-9326/8/1/014003, 2013.

Klimont, Z., Kupiainen, K., Heyes, Ch., Purohit, P., Cofala, J., Rafaj, P., Borken-Kleefeld, J., and Schoepp, W.: Global anthropogenic emissions of particulate matter, in preparation, 2015a.

Klimont, Z., Hoglund, L., Heyes, Ch., Rafaj, P., Schoepp, W., Cofala, J., Borken-Kleefeld, J., Purohit, P., Kupiainen, K., Winiwarter, W., Amann, M., Zhao, B., Wang, S. X., Bertok, I., and Sander, R.: Global scenarios of air pollutants and methane: 1990–2050, in preparation, 2015b.

ACPD
15, 15155–15241, 2015

Knutti, R. and Hegerl, G. C.: The equilibrium sensitivity of the Earth's temperature to radiation changes, Nat. Geosci., 1, 735–753, doi:10.1038/ngeo337, 2008.
Koch, D., Bond, T. C., Streets, D., Unger, N., and van der Werf, G. R.: Global impacts of aerosols from particular source regions and sectors, J. Geophys. Res., 112, D02205, doi:10.1029/2005JD007024, 2007.
Kopp, R. E. and Mauzerall, D. L.: Assessing the climatic benefits of black carbon mitigation, P. Natl. Acad. Sci. USA, 107, 11703–11708, 2010.
Kvalevåg, M. M., Samset, B., and Myhre, G.: Hydrological sensitivity to greenhouse gases and aerosols in a global climate model, Geophys. Res. Lett., 40, 1432–1438, 2013.
Lamarque, J.-F., Bond, T. C., Eyring, V., Granier, C., Heil, A., Klimont, Z., Lee, D., Liousse, C., Mieville, A., Owen, B., Schultz, M. G., Shindell, D., Smith, S. J., Stehfest, E., Van Aardenne, J., Cooper, O. R., Kainuma, M., Mahowald, N., McConnell, J. R., Naik, V., Riahi, K., and van Vuuren, D. P.: Historical (1850–2000) gridded anthropogenic and biomass burning emissions of reactive gases and aerosols: methodology and application, Atmos. Chem. Phys., 10, 7017–7039, doi:10.5194/acp-10-7017-2010, 2010.
Lee, D. S., Fahey, D. W., Forster, P. M., Newton, P. J., Wit, R. C. N., Lim, L. L., Owen, B., and Sausen, R.: Aviation and global climate change in the 21st century, Atmos. Environ., 43, 3520–3537, 2009.
Lelieveld, J., Berresheim, H., Borrmann, S., Crutzen, P. J., Dentener, F. J., Fischer, H., Feichter, J.,Flatau, P. J., Heland, J., Holzinger, R., Korrmann, R., Lawrence, M. G., Levin, Z., Markowicz, K. M., Mihalopoulos, N., Minikin, A., Ramanathan, V., De Reus, M., Roelofs, G. J., Scheeren, H. A., Sciare, J., Schlager, H., Schultz, M., Siegmund, P., Steil, B., Stephanou, E. G., Stier, P., Traub, M., Warneke, C., Williams, J., and Ziereis, H.: Global air pollution crossroads over the Mediterranean, Science, 298, 794–799, 2002.
Lim, S. S., Vos, T., Flaxman, A. D. et al.: A comparative risk assessment of burden of disease and injury attributable to 67 risk factors and risk factor clusters in 21 regions, 1990–2010: a systematic analysis for the Global Burden of Disease Study 2010, Lancet, 380, 2224–2260, doi:10.1016/S0140-6736(12)61766-8, 2012.
Lund, M., Berntsen, T., Fuglestvedt, J., Ponater, M., and Shine, K.: How much information is lost by using global-mean climate metrics? an example using the transport sector, Climatic Change, 113, 949–963, 2012.

ACPD
15, 15155–15241, 2015

Lund, T. M., Berntsen, T. K., Heyes, C., Klimont, Z., and Samset, B. H.: Global and regional climate impacts of black carbon and co-emitted species from the on-road diesel sector, Atmos. Environ., 98, 50–58, 2014a.
Lund, T. M., Berntsen, T. K., and Fuglestvedt, J. S.: Climate impacts of short-lived climate forcers versus CO_2 from biodiesel: a case of the EU on-road sector, Environ. Sci. Technol., 48, 14445–14454, doi:10.1021/es505308g, 2014b.
MacIntosh, C. R., Shine, K. P., and Collins, W. J.: Radiative forcing and climate metrics for ozone precursor emissions: the impact of multi-model averaging, Atmos. Chem. Phys., 15, 3957–3969, doi:10.5194/acp-15-3957-2015, 2015.
Mahowald, N.: Aerosol indirect effect on biogeochemical cycles and climate, Science, 334, 794–796, doi:10.1126/science.1207374, 2011.
Mann, G. W., Carslaw, K. S., Spracklen, D. V., Ridley, D. A., Manktelow, P. T., Chipperfield, M. P., Pickering, S. J., and Johnson, C. E.: Description and evaluation of GLOMAP-mode: a modal global aerosol microphysics model for the UKCA composition-climate model, Geosci. Model Dev., 3, 519–551, doi:10.5194/gmd-3-519-2010, 2010.
Manne, A. S. and Richels, R. G.: An alternative approach to establishing trade-offs among greenhouse gases, Nature, 410, 675–677, 2001.
Meinshausen, M., Meinshausen, N., Hare, W., Raper, S. C. B., Frieler, K., Knutti, R., Frame, D. J., and Allen, M. R.: Greenhouse-gas emission targets for limiting global warming to 2 °C, Nature, 458, 1158–1162, 2009.
Mercado, L. M., Bellouin, N., Sitch, S., Boucher, O., Huntingford, C., Wild, O., and Cox, P. M.: Impact of changes in diffuse radiation on the global land carbon sink, Nature, 458, 1014–1017, doi:10.1038/nature07949, 2009.
Mitchell, T. D. and Jones, P. D.: An improved method of constructing a database of monthly climate observations and associated high-resolution grids, Int. J. Climatol., 25, 693–712, doi:10.1002/joc.1181, 2005.
Molina, M., Zaelke, D., Sarma, K. M., Andersen, S. O., Ramanathan, V., and Kaniaru, D.: Reducing abrupt climate change risk using the Montreal Protocol and other regulatory actions to complement cuts in CO_2 emissions, P. Natl. Acad. Sci. USA, 106, 20616–20621, 2009.
Myhre, G., Berglen, T. F., Johnsrud, M., Hoyle, C. R., Berntsen, T. K., Christopher, S. A., Fahey, D. W., Isaksen, I. S. A., Jones, T. A., Kahn, R. A., Loeb, N., Quinn, P., Remer, L., Schwarz, J. P., and Yttri, K. E.: Modelled radiative forcing of the direct aerosol effect with

ACPD
15, 15155–15241, 2015

multi-observation evaluation, Atmos. Chem. Phys., 9, 1365–1392, doi:10.5194/acp-9-1365-2009, 2009.
Myhre, G., Fuglestvedt, J. S., Berntsen, T. K., and Lund, M. T.: Mitigation of short-lived heating components may lead to unwanted long-term consequences, Atmos. Environ., 45, 6103–6106, doi:10.1016/j.atmosenv.2011.08.009, 2011.
Myhre, G., Shindell, D., Breon, F.-M., Collins, W., Fuglestvedt, J., Huang, J., Koch, D., Lamarque, J.-F., Lee, D., Mendoza, B., Nakajima, T., Robock, A., Stephens, G., Takemura, T., and Zhang, H.: Anthropogenic and natural radiative forcing, in: Climate Change 2013: the Physical Science Basis. Contribution of Working Group I to the Fifth Assessment Report of the Intergovernmental Panel on Climate Change, edited by: Stocker, T. F., Qin, D., Plattner, G.-K., Tignor, M., Allen, S. K., Boschung, J., Nauels, A., Xia, Y., Bex, V., and Midgley, P. M., Cambridge University Press, Cambridge, UK and New York, NY, USA, 659–740, 2013.
Naik, V., Mauzerall, D., Horowitz, L., Schwarzkopf, M. D., Ramaswamy, V., and Oppenheimer, M.: Net radiative forcing due to changes in regional emissions of tropospheric ozone precursors, J. Geophys. Res., 110, D24306, doi:10.1029/2005JD005908, 2005.
Olivié, D. J. L. and Peters, G. P.: Variation in emission metrics due to variation in CO_2 and temperature impulse response functions, Earth Syst. Dynam., 4, 267–286, doi:10.5194/esd-4-267-2013, 2013.
Orlowsky, B. and Seneviratne, S. I.: Global changes in extreme events: regional and seasonal dimension, Climatic Change, 110, 669–696, doi:10.1007/s10584-011-0122-9, 2012.
Penner, J. E., Prather, M. J., Isaksen, I. S. A., Fuglestvedt, J. S., Klimont, Z., and Stevenson, D. S.: Short-lived uncertainty?, Nat. Geosci., 3, 587–588, doi:10.1038/ngeo932, 2010.
Pierrehumbert, R. T.: Short-Lived Climate Pollution, Annu. Rev. Earth Pl. Sc., 42, 341–379, doi:10.1146/annurev-earth-060313-054843, 2014.
Pope III, C. A., Thun, M. J., Namboodiri, M. M., Dockery, D. W., Evans, J. S., and Speizer, F. E.: Particulate air pollution as a predictor of mortality in a prospective study of U.S. adults, Am. J. Resp. Crit. Care, 151, 669–674, 1995.
Pope III, C. A., Burnett, R. T., Thun, M. J., Calle, E. E., Krewski, D., Ito, K., and Thurston, G. D.: Lung cancer, cardiopulmonary mortality, and long-term exposure to fine particulate air pollution, JAMA-J. Am. Med. Assoc., 287, 1132–1141, 2002.
Pope III, C. A., Ezzati, M., and Dockery, D. W.: Fine-particulate air pollution and life expectancy in the United States, New Engl. J. Med., 360, 376–386, doi:10.1056/NEJMsa0805646, 2009.

ACPD
15, 15155–15241, 2015

Prather, M. J., Holmes, C. D., and Hsu, J.: Reactive greenhouse gas scenarios: systematic exploration of uncertainties and the role of atmospheric chemistry, Geophys. Res. Lett., 39, L09803, doi:10.1029/2012GL051440, 2012.

Quaas, J., Ming, Y., Menon, S., Takemura, T., Wang, M., Penner, J. E., Gettelman, A., Lohmann, U., Bellouin, N., Boucher, O., Sayer, A. M., Thomas, G. E., McComiskey, A., Feingold, G., Hoose, C., Kristjánsson, J. E., Liu, X., Balkanski, Y., Donner, L. J., Ginoux, P. A., Stier, P., Grandey, B., Feichter, J., Sednev, I., Bauer, S. E., Koch, D., Grainger, R. G., Kirkevåg, A., Iversen, T., Seland, Ø., Easter, R., Ghan, S. J., Rasch, P. J., Morrison, H., Lamarque, J.-F., Iacono, M. J., Kinne, S., and Schulz, M.: Aerosol indirect effects – general circulation model intercomparison and evaluation with satellite data, Atmos. Chem. Phys., 9, 8697–8717, doi:10.5194/acp-9-8697-2009, 2009.

Quennehen, B., Raut, J.-C., Law, K. S., Ancellet, G., Clerbaux, C., Kim, S.-W., Lund, M. T., Myhre, G., Olivié, D. J. L., Safieddine, S., Skeie, R. B., Thomas, J. L., Tsyro, S., Bazureau, A., Bellouin, N., Daskalakis, N., Hu, M., Kanakidou, M., Klimont, Z., Kupiainen, K., Myriokefalitakis, S., Quaas, J., Rumbold, S. T., Schulz, M., Cherian, R., Shimizu, A., Wang, J., Yoon, S.-C., and Zhu, T.: Multi-model evaluation of short-lived pollutant distributions over East Asia during summer 2008, Atmos. Chem. Phys. Discuss., 15, 11049–11109, doi:10.5194/acpd-15-11049-2015, 2015.

Quinn, P. K., Bates, T. S., Baum, E., Doubleday, N., Fiore, A. M., Flanner, M., Fridlind, A., Garrett, T. J., Koch, D., Menon, S., Shindell, D., Stohl, A., and Warren, S. G.: Short-lived pollutants in the Arctic: their climate impact and possible mitigation strategies, Atmos. Chem. Phys., 8, 1723–1735, doi:10.5194/acp-8-1723-2008, 2008.

Ramanathan, V. and Carmichael, G.: Global and regional climate changes due to black carbon, Nat. Geosci., 1, 221–222, 2008.

Reddy, M. S. and Boucher, O.: Climate impact of black carbon emitted from energy consumption in the world's regions, Geophys. Res. Lett., 34, L11802, doi:10.1029/2006GL028904, 2007.

Reisinger, A., Maltehausen, M., Manning, M., and Bodeker, G.: Uncertainties of global warming metrics: CO_2 and CH_4, Geophys. Res. Lett., 47, L14707, doi:10.1029/2010GL043803, 2010.

Rogelj, J., Schaeffer, M., Meinshausen, M., Shindell, D. T., Hare, W., Klimont, Z., Velders, G. J. M., Amann, M., and Schellnhuber, H. J.: Disentangling the effects of CO_2 and short-lived climate forcer mitigation, P. Natl. Acad. Sci. USA, 111, 16325–16330, doi:10.1073/pnas.1415631111, 2014.

ACPD
15, 15155–15241, 2015

Rypdal, K., Rive, N., Berntsen, T., Fagerli, H., Klimont, Z., Mideksa, T. K., and Fuglestvedt, J.: Climate and air quality-driven scenarios of ozone and aerosol precursor abatement, Environ. Sci. Policy, 12, 855–869, 2009a.

Rypdal, K., Rive, N., Berntsen, T., Klimont, Z., Mideksa, T. K., Myhre, G., and Bieltvedt Skeie, R.: Costs and global impacts of black carbon abatement strategies, Tellus B, 61, 625–641, 2009b.

Samset, B. H., Myhre, G., Schulz, M., Balkanski, Y., Bauer, S., Berntsen, T. K., Bian, H., Bellouin, N., Diehl, T., Easter, R. C., Ghan, S. J., Iversen, T., Kinne, S., Kirkevåg, A., Lamarque, J.-F., Lin, G., Liu, X., Penner, J. E., Seland, Ø., Skeie, R. B., Stier, P., Takemura, T., Tsigaridis, K., and Zhang, K.: Black carbon vertical profiles strongly affect its radiative forcing uncertainty, Atmos. Chem. Phys., 13, 2423–2434, doi:10.5194/acp-13-2423-2013, 2013.

Samset, B. H., Myhre, G., Herber, A., Kondo, Y., Li, S.-M., Moteki, N., Koike, M., Oshima, N., Schwarz, J. P., Balkanski, Y., Bauer, S. E., Bellouin, N., Berntsen, T. K., Bian, H., Chin, M., Diehl, T., Easter, R. C., Ghan, S. J., Iversen, T., Kirkevåg, A., Lamarque, J.-F., Lin, G., Liu, X., Penner, J. E., Schulz, M., Seland, Ø., Skeie, R. B., Stier, P., Takemura, T., Tsigaridis, K., and Zhang, K.: Modelled black carbon radiative forcing and atmospheric lifetime in AeroCom Phase II constrained by aircraft observations, Atmos. Chem. Phys., 14, 12465–12477, doi:10.5194/acp-14-12465-2014, 2014.

Samset, B. H. and Myhre, G.: Climate response to externally mixed black carbon as a function of altitude, J. Geophys. Res.-Atmos., 120, 2913–2927, doi:10.1002/2014JD022849, 2015.

Schmale, J., Shindell, D., von Schneidemesser, E., Chabay, I., and Lawrence, M.: Air pollution: clean up our skies, Nature, 515, 335–337, 2014.

Shindell, D. and Faluvegi, G.: Climate response to regional radiative forcing during the twentieth century, Nat. Geosci., 2, 294–300, doi:10.1038/ngeo473, 2009.

Shindell, D. T., Chin, M., Dentener, F., Doherty, R. M., Faluvegi, G., Fiore, A. M., Hess, P., Koch, D. M., MacKenzie, I. A., Sanderson, M. G., Schultz, M. G., Schulz, M., Stevenson, D. S., Teich, H., Textor, C., Wild, O., Bergmann, D. J., Bey, I., Bian, H., Cuvelier, C., Duncan, B. N., Folberth, G., Horowitz, L. W., Jonson, J., Kaminski, J. W., Marmer, E., Park, R., Pringle, K. J., Schroeder, S., Szopa, S., Takemura, T., Zeng, G., Keating, T. J., and Zuber, A.: A multi-model assessment of pollution transport to the Arctic, Atmos. Chem. Phys., 8, 5353–5372, doi:10.5194/acp-8-5353-2008, 2008.

ACPD
15, 15155–15241, 2015

Shindell, D., Schulz, M., Ming, Y., Takemura, T., Faluvegi, G., and Ramaswamy, R.: Spatial scales of climate response to inhomogeneous radiative forcing, J. Geophys. Res., 115, D19110, doi:10.1029/2010JD014108, 2010.

Shindell, D., Kuylenstierna, J. C. I., Vignati, E., van Dingenen, R., Amann, M., Klimont, Z., Anenberg, S. C., Muller, N., Janssens-Maenhout, G., Raes, F., Schwartz, J., Faluvegi, G., Pozzoli, L., Kupiainen, K., Höglund-Isaksson, L., Emberson, L., Streets, D., Ramanathan, V., Hicks, K., Kim Oanh, N. T., Milly, G., Williams, M., Demkine, V., and Fowler, D.: Simultaneously mitigating near-term climate change and improving human health and food security, Science, 335, 183–189, doi:10.1126/science.1210026, 2012.

Shine, K. P.: The global warming potential: the need for an interdisciplinary retrial. An editorial comment, Climatic Change, 96, 467–472, 2009.

Shine, K. P., Berntsen, T. K., Fuglestvedt, J. S., and Sausen, R.: Scientific issues in the design of metrics for inclusion of oxides of nitrogen in global climate agreements, P. Natl. Acad. Sci. USA, 102, 15768–15773, 2005.

Shine, K. P., Berntsen, T. K., Fuglestvedt, J. S., Bieltvedt Skeie, R., and Stuber, N.: Comparing the climate effect of emissions of short- and long-lived climate agents, Philos. T. R. Soc. A, 365, 1903–1914, 2007.

Shine, K. P., Allan, R. P., Collins, W. J., and Fuglestvedt, J. S.: Metrics for linking emissions of gases and aerosols to global precipitation changes, Earth Syst. Dynam. Discuss., 6, 719–760, doi:10.5194/esdd-6-719-2015, 2015.

Simpson, D., Benedictow, A., Berge, H., Bergström, R., Emberson, L. D., Fagerli, H., Flechard, C. R., Hayman, G. D., Gauss, M., Jonson, J. E., Jenkin, M. E., Nyíri, A., Richter, C., Semeena, V. S., Tsyro, S., Tuovinen, J.-P., Valdebenito, Á., and Wind, P.: The EMEP MSC-W chemical transport model – technical description, Atmos. Chem. Phys., 12, 7825–7865, doi:10.5194/acp-12-7825-2012, 2012.

Sitch, S., Cox, P. M., Collins, W. J., and Huntingford, C.: Indirect radiative forcing of climate change through ozone effects on the land-carbon sink, Nature, 448, 791–794, 2007.

Skeie, R. B., Berntsen, T. K., Myhre, G., Tanaka, K., Kvalevåg, M. M., and Hoyle, C. R.: Anthropogenic radiative forcing time series from pre-industrial times until 2010, Atmos. Chem. Phys., 11, 11827–11857, doi:10.5194/acp-11-11827-2011, 2011.

Skeie, R. B., Berntsen, T., Aldrin, M., Holden, M., and Myhre, G.: A lower and more constrained estimate of climate sensitivity using updated observations and detailed radiative forcing time series, Earth Syst. Dynam., 5, 139–175, doi:10.5194/esd-5-139-2014, 2014.

ACPD
15, 15155–15241, 2015

Skodvin, T. and Fuglestvedt, J. S.: A comprehensive approach to climate change: political and scientific considerations, Ambio, 26, 351–358, 1997.
Smith, S. J., Edmonds, J., Hartin, C. A., Mundra, A., and Calvin, K.: Near-term acceleration in the rate of temperature change, Nature Climate Change, 5, 333–336, doi:10.1038/nclimate2552, 2015.
Stevens, B., Giorgetta, M., Esch, M., Mauritsen, T., Crueger, T., Rast, S., Salzmann, M., Schmidt, H., Bader, J., Block, K., Brokopf, R., Fast, I., Kinne, S., Kornblueh, L., Lohmann, U., Pincus, R., Reichler, T., and Roeckner, E.: Atmospheric component of the MPI-M Earth System Model: ECHAM6-HAM2, J. Adv. Model. Earth Sy., 5, 146–172, doi:10.1002/jame.20015, 2013.
Stjern, C. W., Stohl, A., and Kristjánsson, J. E.: Have aerosols affected trends of visibility and precipitation in Europe?, J. Geophys. Res., 116, D02212, doi:10.1029/2010JD014603, 2011.
Stohl, A. and Trickl, T.: A textbook example of long-range transport: simultaneous observation of ozone maxima of stratospheric and North American origin in the free troposphere over Europe, J. Geophys. Res., 104, 30445–30462, 1999.
Stohl, A., Hittenberger, M., and Wotawa, G.: Validation of the Lagrangian particle dispersion model FLEXPART against large scale tracer experiments, Atmos. Environ., 32, 4245–4264, 1998.
Stohl, A., Forster, C., Frank, A., Seibert, P., and Wotawa, G.: Technical note: The Lagrangian particle dispersion model FLEXPART version 6.2, Atmos. Chem. Phys., 5, 2461–2474, doi:10.5194/acp-5-2461-2005, 2005.
Stohl, A., Klimont, Z., Eckhardt, S., Kupiainen, K., Shevchenko, V. P., Kopeikin, V. M., and Novigatsky, A. N.: Black carbon in the Arctic: the underestimated role of gas flaring and residential combustion emissions, Atmos. Chem. Phys., 13, 8833–8855, doi:10.5194/acp-13-8833-2013, 2013.
Tanaka, K., O'Neill, B. C., Rokityanskiy, D., Obersteiner, M., and Tol, R. S. J.: Evaluating Global Warming Potentials with historical temperature, Climatic Change, 96, 443–466, 2009.
Tanaka, K., Johansson, D. J. A., O'Neill, B. C., and Fuglestvedt, J. S.: Emission metrics under the 2 °C climate stabilization target, Climatic Change, 117, 933–941, doi:10.1007/s10584-013-0693-8, 2013.
Taylor, K. E., Stouffer, R. J., and Meehl, G. A.: An overview of CMIP5 and the experiment design, B. Am. Meteorol. Soc., 93, 485–498, doi:10.1175/BAMS-D-11-00094.1, 2012.

ACPD
15, 15155–15241, 2015

Tragou, E. and Lascaratos, A.: Role of aerosols on the Mediterranean solar radiation, J. Geophys. Res., 108, 3025, doi:10.1029/2001JC001258, 2003.
Tsigaridis, K., Daskalakis, N., Kanakidou, M., Adams, P. J., Artaxo, P., Bahadur, R., Balkanski, Y., Bauer, S. E., Bellouin, N., Benedetti, A., Bergman, T., Berntsen, T. K., Beukes, J. P., Bian, H., Carslaw, K. S., Chin, M., Curci, G., Diehl, T., Easter, R. C., Ghan, S. J., Gong, S. L., Hodzic, A., Hoyle, C. R., Iversen, T., Jathar, S., Jimenez, J. L., Kaiser, J. W., Kirkevåg, A., Koch, D., Kokkola, H., Lee, Y. H, Lin, G., Liu, X., Luo, G., Ma, X., Mann, G. W., Mihalopoulos, N., Morcrette, J.-J., Müller, J.-F., Myhre, G., Myriokefalitakis, S., Ng, N. L., O'Donnell, D., Penner, J. E., Pozzoli, L., Pringle, K. J., Russell, L. M., Schulz, M., Sciare, J., Seland, Ø., Shindell, D. T., Sillman, S., Skeie, R. B., Spracklen, D., Stavrakou, T., Steenrod, S. D., Takemura, T., Tiitta, P., Tilmes, S., Tost, H., van Noije, T., van Zyl, P. G., von Salzen, K., Yu, F., Wang, Z., Wang, Z., Zaveri, R. A., Zhang, H., Zhang, K., Zhang, Q., and Zhang, X.: The AeroCom evaluation and intercomparison of organic aerosol in global models, Atmos. Chem. Phys., 14, 10845–10895, doi:10.5194/acp-14-10845-2014, 2014.
UNEP/WMO: Integrated Assessment of Black Carbon and Tropospheric Ozone, United Nations Environment Programme (UNEP), Nairobi, Kenya, 2011.
Unger, N., Bond, T. C., Wang, J. S., Koch, D. M., Menon, S., Shindell, D. T., and Bauer, S.: Attribution of climate forcing to economic sectors, P. Natl. Acad. Sci. USA, 107, 3382–3387, 2010.
van der Werf, G. R., Randerson, J. T., Giglio, L., Collatz, G. J., Mu, M., Kasibhatla, P. S., Morton, D. C., DeFries, R. S., Jin, Y., and van Leeuwen, T. T.: Global fire emissions and the contribution of deforestation, savanna, forest, agricultural, and peat fires (1997–2009), Atmos. Chem. Phys., 10, 11707–11735, doi:10.5194/acp-10-11707-2010, 2010.
Wang, S. X., Zhao, B., Cai, S. Y., Klimont, Z., Nielsen, C. P., Morikawa, T., Woo, J. H., Kim, Y., Fu, X., Xu, J. Y., Hao, J. M., and He, K. B.: Emission trends and mitigation options for air pollutants in East Asia, Atmos. Chem. Phys., 14, 6571–6603, doi:10.5194/acp-14-6571-2014, 2014.
Wang, R., Balkanski, Y., Boucher, O., Ciais, P., Penuelas, J., and Tao, S.: Significant contribution of combustion-related emissions to the atmospheric phosphorus budget, Nat. Geosci., 8, 48–54, doi:10.1038/ngeo2324, 2015.
West, J. J., Fiore, A. M., Horowitz, L. W., and Mauzerall, D. L.: Global health benefits of mitigating ozone pollution with methane emission controls, P. Natl. Acad. Sci. USA, 103, 3988–3993, 2006.

ACPD
15, 15155–15241, 2015

WHO: WHO Air quality guidelines for particulate matter, ozone, nitrogen dioxide and sulfur dioxide: Global update 2005 – Summary of risk assessment, available at: http://www.euro.who.int/__data/assets/pdf_file/0005/78638/E90038.pdf?ua=1 (last access: 22 April 2014), 2006.

WHO: Health effects of black carbon, Joint WHO/UNECE Task Force on Health Aspects of Air Pollutants under UNECE's Long-Range Transboundary Air Pollution Convention (LRTAP), World Health Organization, Regional Office for Europe, Copenhagen, available at: http://www.unece.org/fileadmin/DAM/env/documents/2012/air/Health_Effects_of_Black_Carbon_report.pdf, (last access: 14 May 2013), 2012.

WHO: Review of evidence on health aspects of air pollution – REVIHAAP project: final technical report, available at: http://www.euro.who.int/en/health-topics/environment-and-health/air-quality/publications/2013/review-of-evidence-on-health-aspects-of-air-pollution-revihaap-project-final-technical-report, (last access: 29 April 2014), 2013.

Wild, O., Prather, M. J., and Akimoto, H.: Indirect long-term global radiative cooling from NO_x emissions, Geophys. Res. Lett., 28, 1719–1722, 2001.

Yttri, K. E., Lund Myhre, C., Eckhardt, S., Fiebig, M., Dye, C., Hirdman, D., Ström, J., Klimont, Z., and Stohl, A.: Quantifying black carbon from biomass burning by means of levoglucosan – a one-year time series at the Arctic observatory Zeppelin, Atmos. Chem. Phys., 14, 6427–6442, doi:10.5194/acp-14-6427-2014, 2014.

Zaveri, R. A., Easter, R. C., Fast, J. D., and Peters, L. K.: Model for Simulating Aerosol Interactions and Chemistry (MOSAIC), J. Geophys. Res., 113, D13204, doi:10.1029/2007jd008782, 2008.

Zhang, K., O'Donnell, D., Kazil, J., Stier, P., Kinne, S., Lohmann, U., Ferrachat, S., Croft, B., Quaas, J., Wan, H., Rast, S., and Feichter, J.: The global aerosol-climate model ECHAM-HAM, version 2: sensitivity to improvements in process representations, Atmos. Chem. Phys., 12, 8911–8949, doi:10.5194/acp-12-8911-2012, 2012.

Zhao, B., Wang, S. X., Liu, H., Xu, J. Y., Fu, K., Klimont, Z., Hao, J. M., He, K. B., Cofala, J., and Amann, M.: NO_x emissions in China: historical trends and future perspectives, Atmos. Chem. Phys., 13, 9869–9897, doi:10.5194/acp-13-9869-2013, 2013.

ACPD
15, 15155–15241, 2015

Table 1. Air quality standards for Europe (European Union reference values), WHO air quality guidelines (AQG), US-EPA National Ambient Air Quality Standards (NAAQS) and the Environmental Quality Standards (EQS) and guideline values for air pollutants in Japan. Values in brackets give time period for which the guideline is defined.

Pollutants	EU reference levels[a]	WHO AQG[b]	USEPA NAAQS[c]	Japan EQS[d]
$PM_{2.5}$	20 $\mu g\,m^{-3}$ (year)	10 $\mu g\,m^{-3}$ (year)	12 $\mu g\,m^{-3}$ (year)	15 $\mu g\,m^{-3}$ (year)
PM_{10}	4 $\mu g\,m^{-3}$ (day)	20 $\mu g\,m^{-3}$ (year)	150 $\mu g\,m^{-3}$ (day)	100 $\mu g\,m^{-3}$ (day, SPM[e])
O_3	120 $\mu g\,m^{-3}$ (8 h)	100 $\mu g\,m^{-3}$ (8 h)	0.075 ppm (8 h)	118 $\mu g\,m^{-3}$ (1 h[f])
NO_2	40 $\mu g\,m^{-3}$ (year)	40 $\mu g\,m^{-3}$ (year)	53 ppb (year)	75–113 $\mu g\,m^{-3}$ (1 h)
SO_2	125 $\mu g\,m^{-3}$ (day)	20 $\mu g\,m^{-3}$ (day)	75 ppb (1 h)	105 $\mu g\,m^{-3}$ (1 day)
CO	10 $mg\,m^{-3}$ (8 h)	10 $mg\,m^{-3}$ (8 h)	9 ppm (8 h)	10 ppm (1 h)

[a] EEA 2013, Indicator CSI 004.
[b] WHO Air Quality Guidelines (WHO, 2006).
[c] US-EPA National Ambient Air Quality Standards (http://www.epa.gov/air/criteria.html#3, last access: 16 April 2014).
[d] Environmental Quality Standards (EQS) and guideline values for air pollutants in Japan (Kawamoto et al., 2011).
[e] 100 % efficiency cut-off at 10 µm while PM_{10} is defined as 50 % efficiency cut-off at 10 µm aerodynamic diameter (Kawamoto et al., 2011).
[f] Photochemical oxidants (O_x) (Kawamoto et al., 2011).

ACPD
15, 15155–15241, 2015

Table 2. Overview of the ECLIPSE models and how they were set up for the years 2008–2009.

Model Name	Model Type*	Horizontal/vertical resolution	Meteorological fields	Periods simulated/output temporal resolution	References
FLEXPART	LPDM	Meteorological input 1° × 1°, 92L	ECMWF Operational Analyses	2008–2009, 3 h	Stohl et al. (1998, 2005)
OsloCTM2	CTM	2.8° × 2.8°, 60L	ECMWF Operational Analyses	2008–2009, 3 h	Myhre et al. (2009), Skeie et al. (2011)
EMEP	CTM	1° × 1°, 20L	ECMWF operational	2008–2009, 24 h	Simpson et al. (2012)
TM4-ECPL	CTM	2° × 3°, 34L	ECMWF ERA-interim	2008–2009, 24 h	Kanakidou et al. (2012), Daskalakis et al. (2015)
WRF-CMAQ	CTM	50 km × 50 km, 23L	NCEP	2008, 24 h	Im et al. (2013)
WRF-Chem	CTM	50 km × 50 km, 49L	Nudged to FNL	Mar–Aug 2008, 3 h	Grell et al. (2005), Zaveri et al. (2008)
NorESM	ESM	1.9° × 2.5°, 26L	Internal, observed SST prescribed	2008–2009, 3 h	Kirkevåg et al. (2013), Bentsen et al. (2013)
ECHAM6-HAM2	ESM	1.8° × 1.8°, 31L	ECMWF Reanalysis	Mar–Aug 2008, 1 h	Stevens et al. (2013), Zhang et al. (2012)
HadGEM3	ESM	1.9° × 1.3°, 63L	ECMWF ERA-interim	Mar–Jun, Nov 2008, Jan, May and Nov 2009, 2 h	Hewitt et al. (2011), Mann et al. (2010)
CESM-CAM4	ESM	1.9° × 2.5°, 26L	Internal	Was not evaluated for 2008–2009; only used for 2000–2050 simulations	Gent et al. (2011)

* Chemistry transport model (CTM), Lagrangian particle dispersion model (LPDM), Earth system model (ESM).

ACPD
15, 15155–15241, 2015

Table 3. Top-17 mitigation measures contributing together more than 80 % of the climate benefit. Measures are ranked by importance starting from the top. Methane measures contribute about 47 % of the benefits according to the GTP_{20} metric, while 33 % are attributed to BC focused measures; 20 % are contributed by measures not listed here.

Methane measures	Measures targeting BC reduction
Oil and gas industry: Recovery and use (rather than venting or flaring) of associated gas	Oil and gas industry: Improving efficiency and reducing gas flaring
Oil and gas industry (unconventional): Reducing emissions from unintended leaks during production (extraction) of shale gas	Transport: Eliminating high emitting vehicles (super-emitters)
Coal mining: Reducing (oxidizing) emissions released during hard coal mining (ventilation air CH_4)	Residential-commercial: Clean biomass cooking stoves
Waste: Municipal waste – waste paper separation, collection, and recycling	Residential-commercial: Replacement of kerosene wick lamps with LED lamps
Waste: Municipal food waste separation, collection and treatment in anaerobic digestion (biogasification) plants	Transport: Widespread Euro VI emission standards (incl. particle filters) on diesel vehicles
Coal mining: Hard and brown coal -pre-mining emissions – Degasification	Industrial processes: Modernized (mechanized) coke ovens
Gas distribution: Replacement of grey cast iron gas distribution network	Agriculture: Effective ban of open field burning of agricultural residues
Waste: Industrial solid waste (food, wood, pulp and paper, textile) – recovery and incineration	
Waste: Wastewater treatment from paper and pulp, chemical, and food industries – anaerobic treatment in digester, reactor or deep lagoon with gas recovery, upgrading and use. For residential wastewater centralized collection with anaerobic secondary and/or tertiary treatment (incl. treatment with bacteria and/or flaring of residual CH_4)	
Oil and gas industry (conventional): Reducing emissions from unintended leaks during production (extraction)	

ACPD
15, 15155–15241, 2015

Table 4. Relative differences (%) in O_3 and $PM_{2.5}$ surface concentrations between simulations using the mitigation (MIT) and current legislation (CLE) scenarios (given as $100 \times$ (MIT-CLE)/CLE) for several regions and for the final decade of the simulations (2041–2050). The regions correspond to the boxes shown in Fig. 10. Except for the Mediterranean, only the land-based grid cells inside the boxes were used. Mean values and full model ranges for the three models NorESM, HadGEM and OsloCTM2 are reported. To exclude effects of changes in sea salt and dust emissions caused by natural variability and emission responses to forced changes in meteorological conditions, sea salt and dust concentrations were kept at CLE levels for the purpose of these calculations.

Region	O_3 mean (%)	O_3 range (%)	$PM_{2.5}$ mean (%)	$PM_{2.5}$ range (%)
Northern Europe	−13.7	[−15.9, −11.1]	−12.5	[−17.6, −7.3]
Southern Europe	−14.9	[−17.0, −12.3]	−2.3	[−3.1, −1.5]
Mediterranean	−15.1	[−17.8, −12.6]	−1.6	[−2.3, −1.0]
Eastern China	−19.3	[−24.4, −16.0]	−16.3	[−23.2, −11.8]
Western China	−15.8	[−17.9, −12.8]	−2.2	[−4.3, −1.0]
India	−17.1	[−22.8, −12.7]	−19.8	[−22.5, −17.9]
Eastern United States	−13.6	[−15.7, −10.3]	−8.8	[−11.7, −3.6]
Western United States	−14.3	[−16.1, −11.5]	−4.5	[−8.7, −1.4]

ACPD
15, 15155–15241, 2015

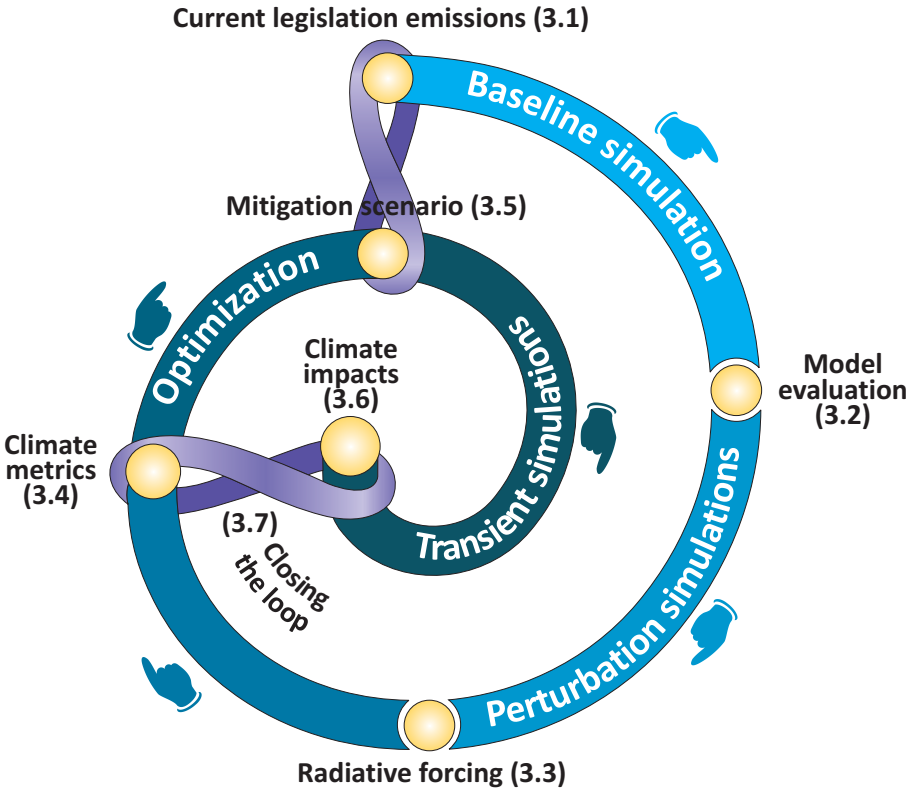

Figure 1. Schematic of the ECLIPSE overall methodology. Numbers in brackets correspond to section numbers in this paper.

ACPD
15, 15155–15241, 2015

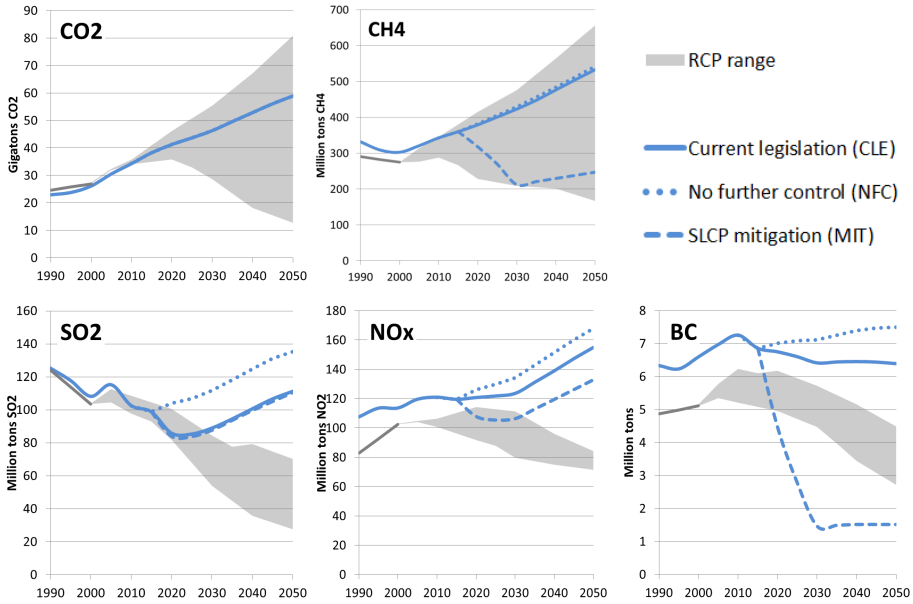

Figure 2. Global annual anthropogenic emissions of CO_2, CH_4 and key air pollutants (SO_2, NO_x and BC) for the current legislation (CLE), no further controls (NFC) and ECLIPSE SLCP mitigation scenario. Units are Gt for CO_2 and Mt for the SLCPs. Also shown for comparison is the range of the RCP emission scenarios (grey shading).

ACPD
15, 15155–15241, 2015

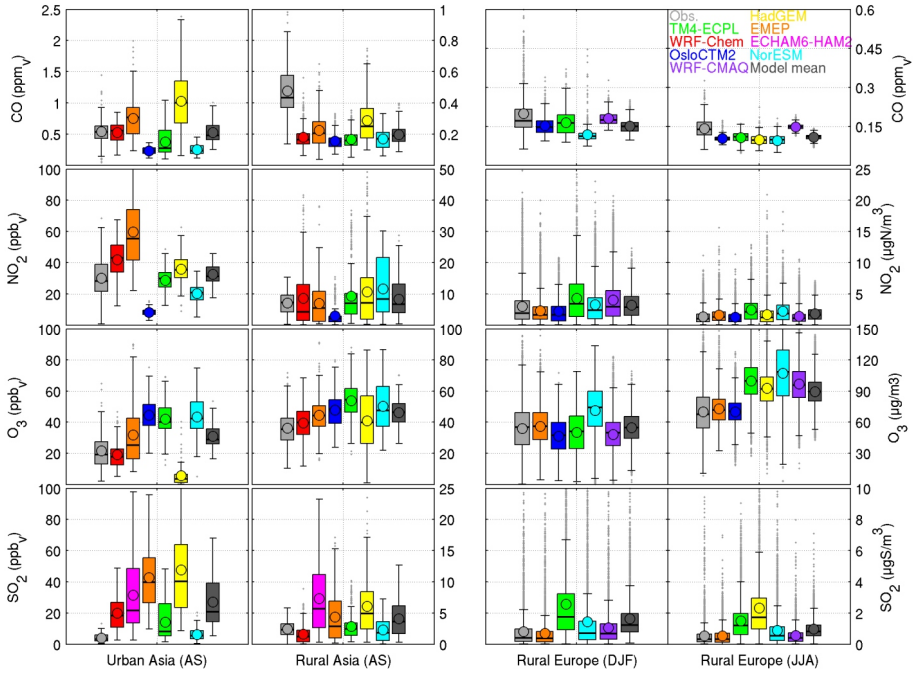

Figure 3. Box and whiskers plots showing the frequency distribution of measured and modelled CO, NO_2, O_3 and SO_2 mixing ratios or concentrations representative for background stations in urban and rural areas in East Asia during August and September 2008 (two left panel columns) and for rural background stations in Europe for winter (December–February, DJF) and summer (June–August, JJA) 2008 (two right panel columns). Circles and central lines show the means and the medians, respectively; box edges represent the 25th and the 75th percentiles. For East Asia, results are averaged over several sites: Beijing, Inchon and Seoul for the urban areas, Gosan, Kunsan, Kangwha, Mokpo and Taean for rural areas. Results for individual sites can be found in Quennehen et al. (2015). For Europe, daily mean observed values are averaged over all stations of the EMEP network with available data. Model data are treated like the observations and only the days with available observations are taken into account.

ACPD
15, 15155–15241, 2015

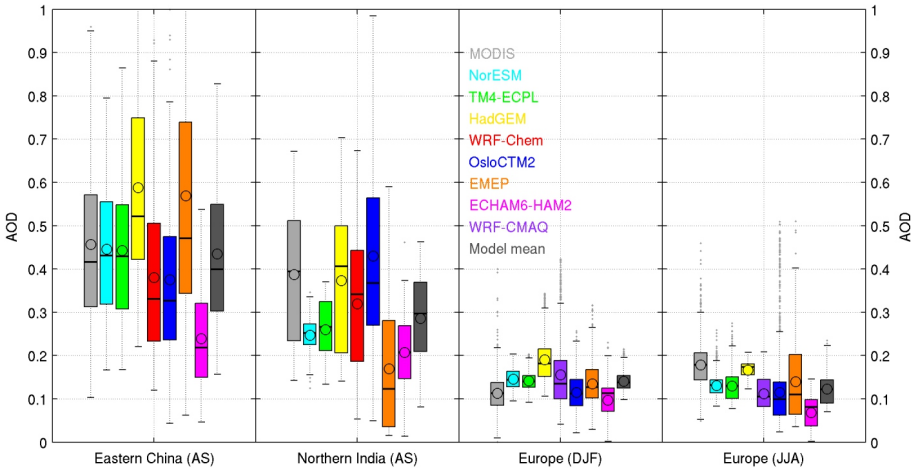

Figure 4. Comparison of satellite-derived (MODIS) and modelled aerosol optical depth (AOD) at wavelengths of 550 nm over Eastern China and Northern India (for area definition, see Quennehen et al., 2015) in August–September 2008, and Europe (14.5° W–34.5° E, 35.5–74.5° N) in winter (December–February, DJF) and summer (June–August, JJA) of 2008. Mean values (circles), medians (central lines), 25th and 75th percentiles (boxes) and range of other data excluding outliers (whiskers) are shown.

ACPD
15, 15155–15241, 2015

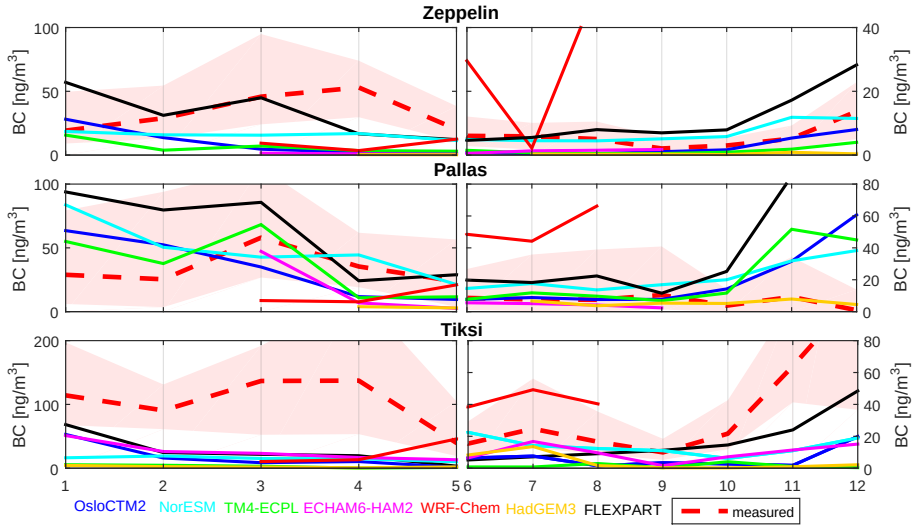

Figure 5. Monthly (month is displayed on the abscissa) median observed and modelled BC concentrations for the stations Zeppelin on Svalbard (11.9° E, 78.9° N, top), Pallas in Finland (24.12° E, 67.97° N, middle) and Tiksi in Siberia (128.9° E, 71.6° N, bottom), for late winter/spring (left column) and summer/autumn (right column) for the years 2008–2009 (for Tiksi, measured values were available only from July 2009 to June 2010). The red dashed lines connect the observed median values, the light red shaded areas span from the 25th to the 75th percentile of the observations. Modelled median values are shown with lines of different colour according to the legend. Notice that different concentration scales are used for individual panels and also for January–May (axis on left hand side) and June–December (axis on right hand side) periods. Modified from Eckhardt et al. (2015).

ACPD
15, 15155–15241, 2015

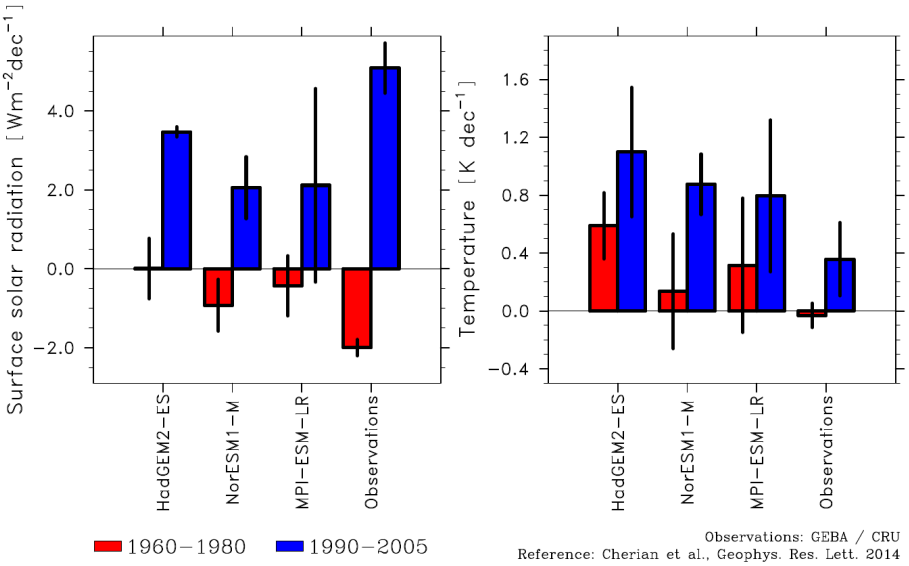

Figure 6. Linear trends in (left) surface solar radiation and (right) near-surface temperature increase per decade over continental Europe from the "historical" simulations in the CMIP5 archive contributed by previous versions of three ECLIPSE ESMs. The period 1960–1980 is shown in red, the period 1990–2005 in blue.

ACPD
15, 15155–15241, 2015

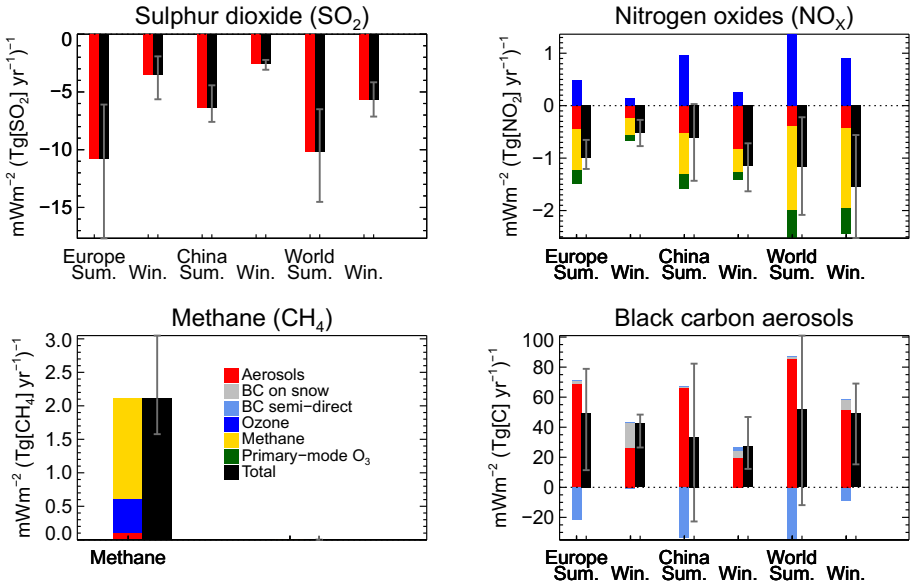

Figure 7. The ECLIPSE estimates of specific radiative forcing (SRF, mW m^{-2} Tg^{-1} yr^{-1} of emission rate change) for reductions in the emissions of SO_2, NO_x, CH_4, and BC aerosols in Europe, China and the global average, separately for NH summer (Sum., May–October) and NH winter (Win., November–April). Shown are values averaged over all five models, with the error bars indicating the full range of the model estimates. Colours indicate the contribution of different forcing mechanisms. Notice that for CH_4 regionality was not accounted for because, due to its longer lifetime, forcing does not depend on the emission region.

ACPD
15, 15155–15241, 2015

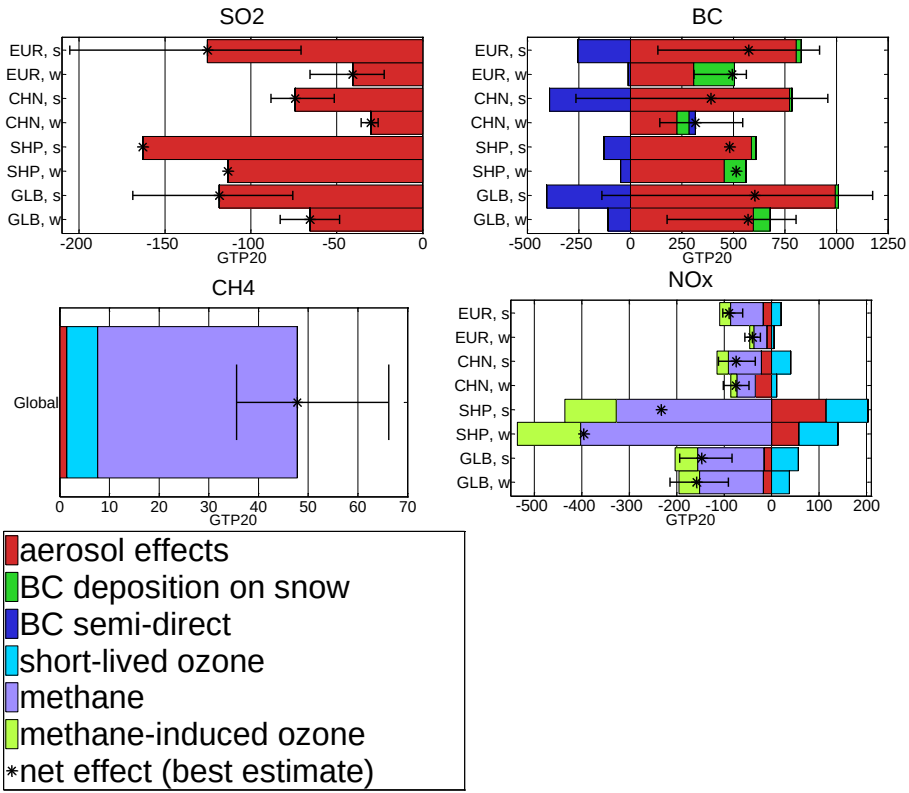

Figure 8. GTP_{20} values for SLCPs, relative to an equal mass emission of CO_2, for all regions and seasons, decomposed by processes and based on the RF values shown in Fig. 7. The regions included are Europe (EUR), China (CHN), global (GLB), and the shipping sector considered separately (SHP), all for both NH summer (s, May–October) and NH winter (w, November–April). Uncertainty bars reflect model spread. Only two models calculated effects of emissions from shipping and there no uncertainty range is given.

ACPD
15, 15155–15241, 2015

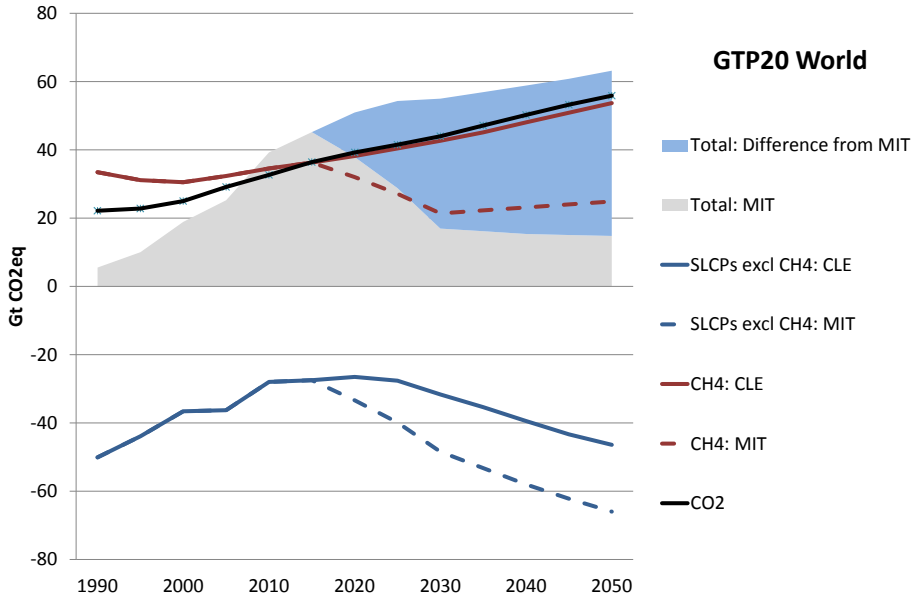

Figure 9. CO_2-equivalent emissions (Gt) determined with the GTP_{20} metric, as a function of time, for global emissions of the current legislation (CLE) and SLCP mitigation (MIT) scenarios. Lines show the values for individual forcing components (black CO_2, red CH_4, blue other SLCPs), while the shaded areas show the total CO_2 equivalent emissions from all SLCPs and CO_2. The blue shading indicates the mitigation potential of MIT, compared to CLE.

ACPD
15, 15155–15241, 2015

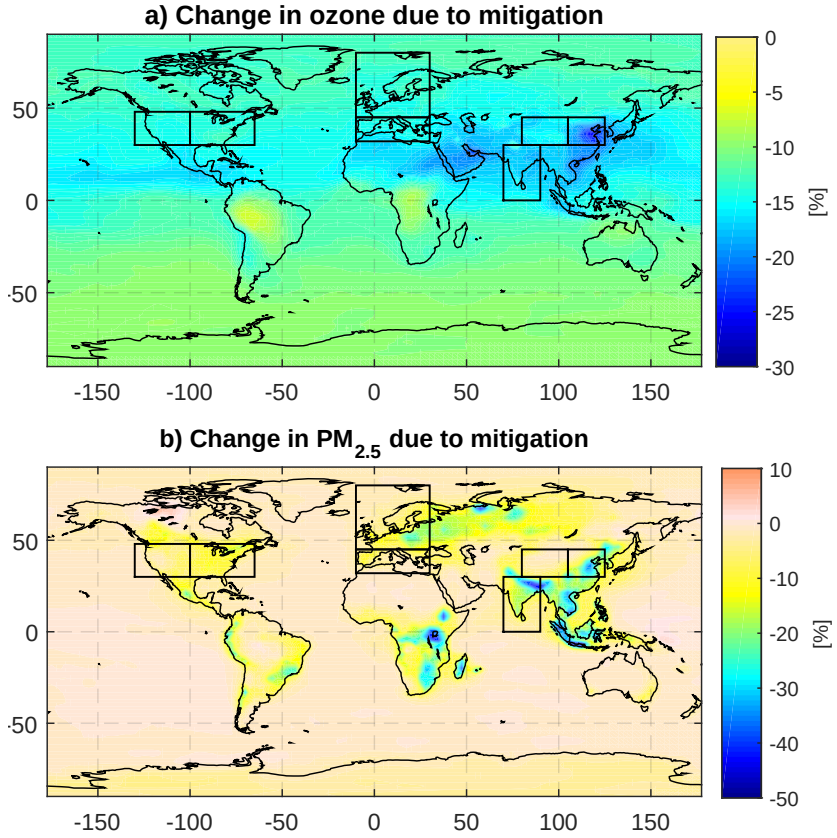

Figure 10. Relative difference maps (in %) for the surface concentrations of O_3 and $PM_{2.5}$, as obtained from simulations based on the emission mitigation (MIT) scenario and the current legislation (CLE) scenario, i.e. (100 × (MIT-CLE)/CLE). Shown are mean concentration differences for the period 2041–2050 and averaged over model results from OsloCTM2, NorESM and HadGEM. The black boxes define the regions used in Table 4.

ACPD
15, 15155–15241, 2015

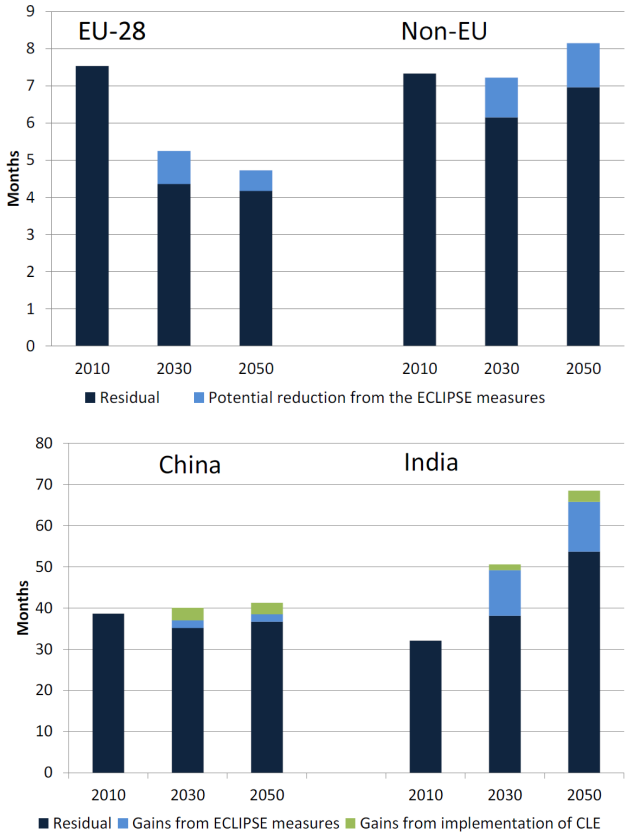

Figure 11. Loss of statistical life expectancy (months) due to the exposure to $PM_{2.5}$ in Europe, for EU-28 and Non-EU countries (upper panel) and for China and India (lower panel). The black bars give the values for the mitigation (MIT) scenario, whereas the blue increments show the difference to the current legislation (CLE) scenario. For India and China, green bars indicate the gains from the implementation of the CLE scenario.

ACPD
15, 15155–15241, 2015

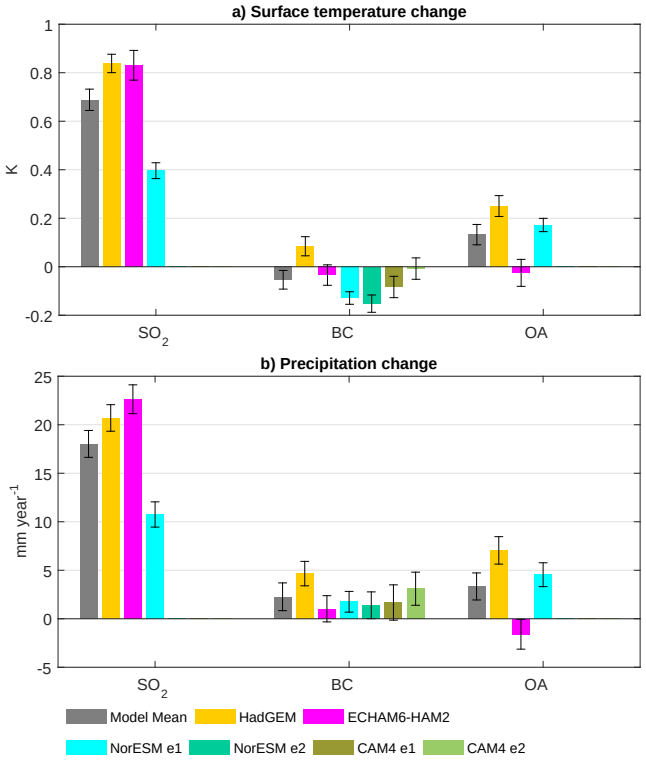

Figure 12. Global mean annual average changes in **(a)** surface temperature and **(b)** precipitation averaged over all land areas excluding ice sheets, from the four ESMs (one was run only for BC), for a complete removal of all land-based emissions of a particular species, compared to the ECLIPSE version 4 baseline emissions for the year 2008 (CESM-CAM4 used the year 2000). The plot shows results averaged over 50 year model simulations; for NorESM and CESM-CAM4, two ensemble members each were run for BC. Error bars are 95 % confidence intervals in the mean, based on 50 annual means from each model and thus only reflect the uncertainty of the mean caused by natural variability within each model.

ACPD
15, 15155–15241, 2015

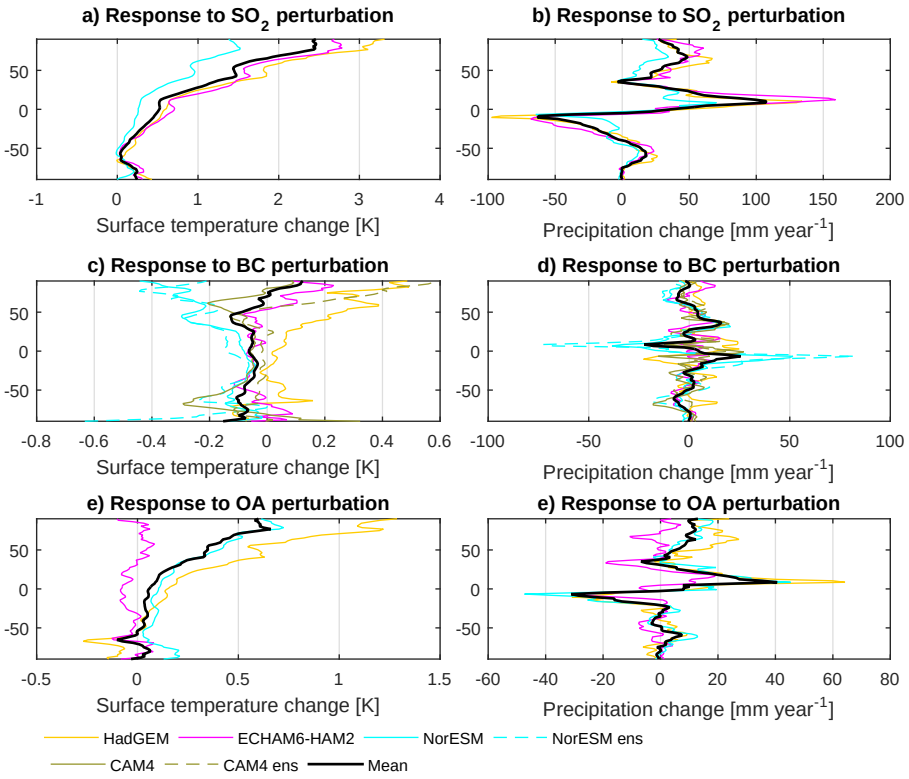

Figure 13. Annual mean changes in zonal-mean surface temperature (left panels **a, c, e**) and precipitation (right panels **b, d, f**) for a complete removal of all land-based emissions of **(a, b)** SO_2, **(c, d)** BC, and **(e, f)** OA. Notice the differences in scales between different panels.

ACPD
15, 15155–15241, 2015

Evaluating the climate and air quality impacts of short-lived pollutants

A. Stohl et al.

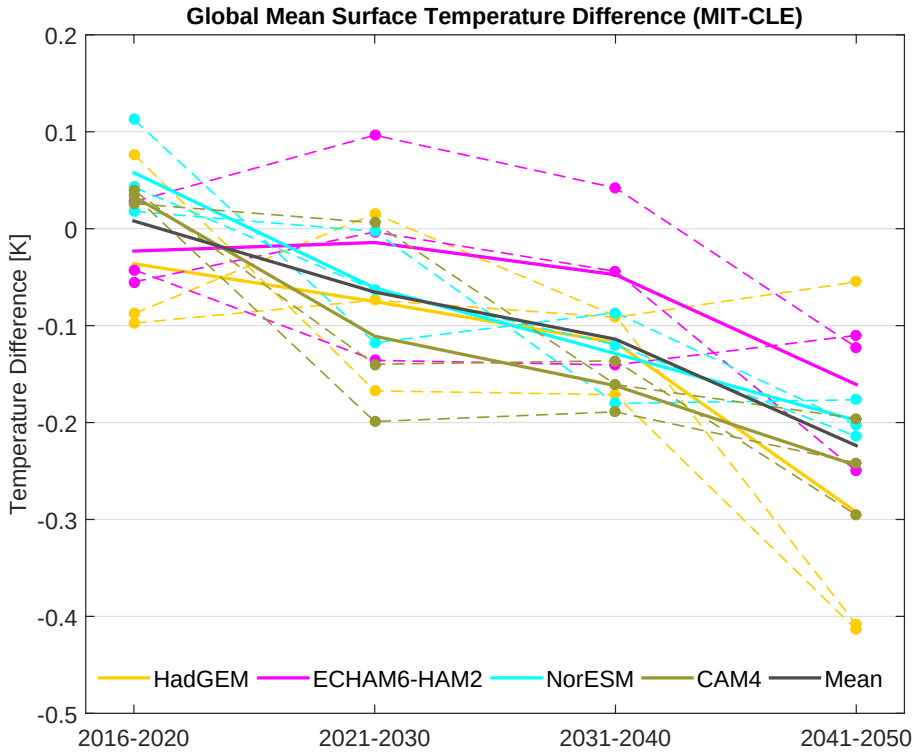

Figure 14. Time evolution of differences in global mean surface temperature between transient simulations following the mitigation (MIT) and the current legislation (CLE) scenario, i.e. (MIT-CLE), for the four ECLIPSE models. Negative values mean that temperatures are lower in the MIT than in the CLE scenario. The ensemble means for each model are shown as thick lines, whereas the individual ensemble members are shown with thin lines.

ACPD
15, 15155–15241, 2015

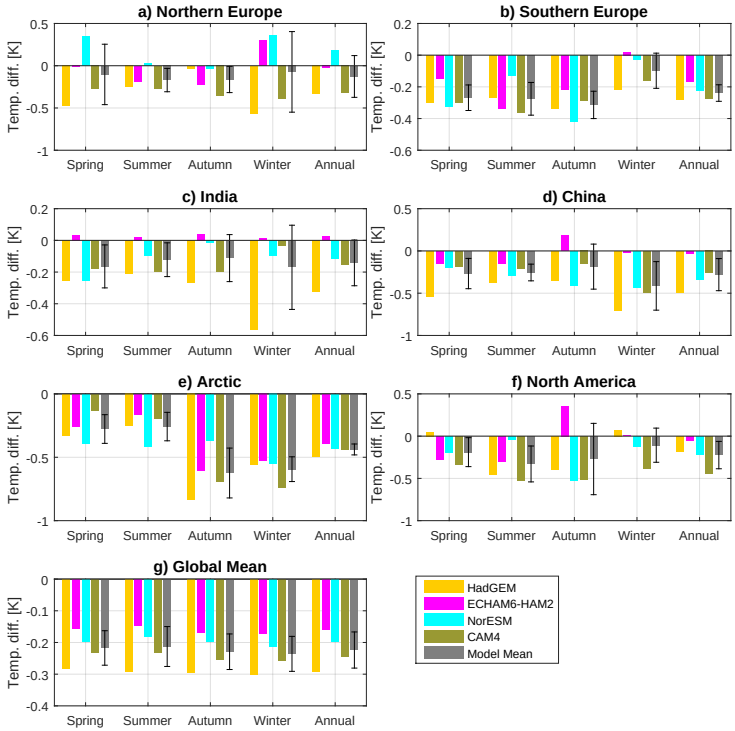

Figure 15. Seasonal and annual mean differences in surface temperatures (in K) in various regions **(a–f)** and for the whole globe **(g)** between transient simulations of the mitigation (MIT) and the current legislation (CLE) scenario, i.e. (MIT-CLE), averaged over the last 10 years of the simulations (2041–2050). Regions are defined as **(a)** 45–65° N, 10° W–65° E, **(b)** 30–45° N, 10° W–65° E, **(c)** 7–35° N, 68–90° E, **(d)** 24–48° N, 80–132° E, **(e)** 60–90° N, **(f)** 30–60° N, 120–50° W. Results are shown for the four ECLIPSE models individually and for the multi-model mean. Negative values mean that temperatures are lower in the MIT than in the CLE scenario. Error bars on the model mean values show the standard deviations of the individual model results.

ACPD
15, 15155–15241, 2015

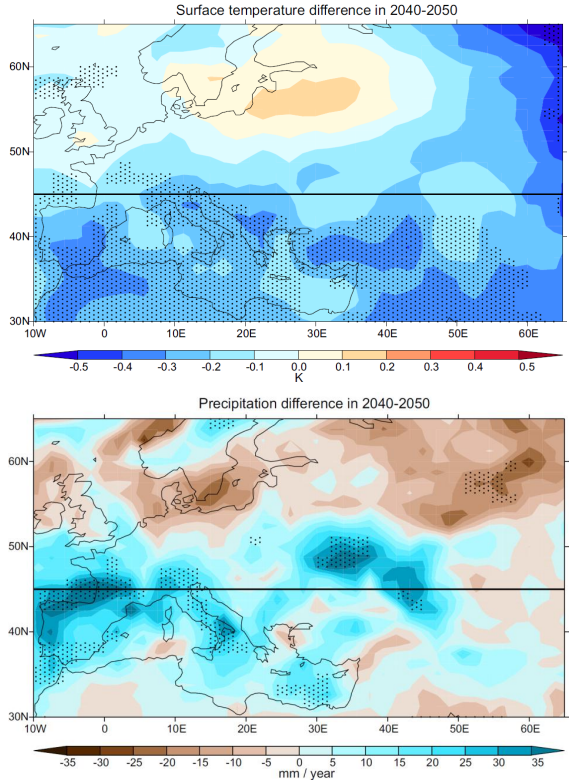

Figure 16. Annual average differences in (top) surface temperature and (bottom) precipitation over Europe between the transient simulations based on the mitigation (MIT) and the current legislation (CLE) scenario, averaged over the last 10 years of the simulations (2041–2050). Stippling shows where all four models agree on the sign of the response. The thick horizontal line distinguishes the southern and northern Europe boxes. In the top panel, negative values mean that temperature in the MIT scenario is lower than in the CLE scenario; in the bottom panel, positive values mean that there is more precipitation in the MIT than in the CLE scenario.

ACPD
15, 15155–15241, 2015

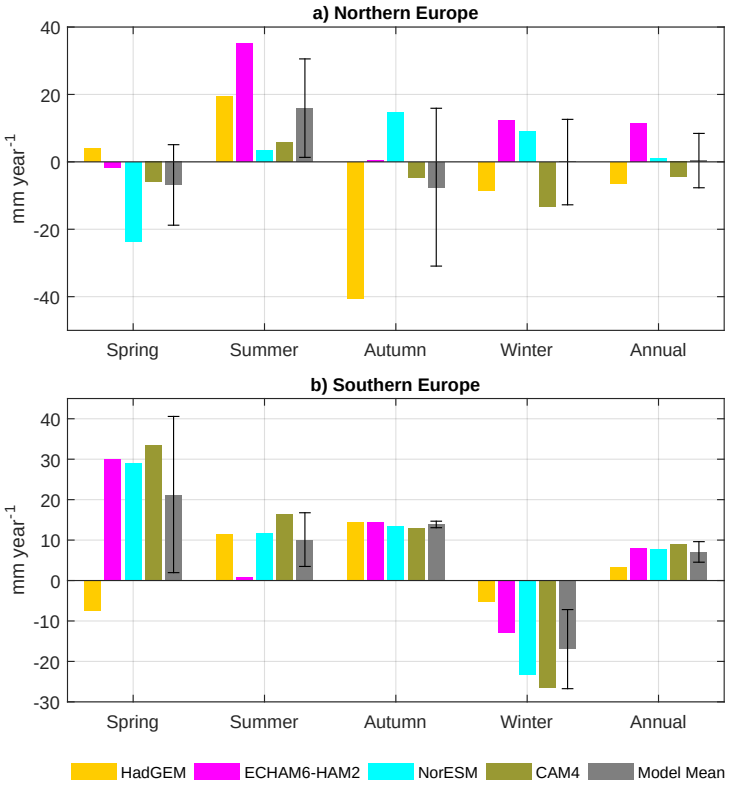

Figure 17. Seasonal and annual mean differences in precipitation (in mm yr^{-1}) over Northern **(a)** and Southern **(b)** Europe between transient simulations of the mitigation (MIT) scenario and the current legislation (CLE) scenario, averaged over the last 10 years of the simulations (2041–2050). Regions are defined as for Fig. 15a and b. Results are shown for the four ECLIPSE models individually and for the multi-model mean. Positive values mean that MIT simulations have more precipitation than CLE simulations. Error bars on the model mean values show the standard deviations of the individual model results.

ACPD
15, 15155–15241, 2015

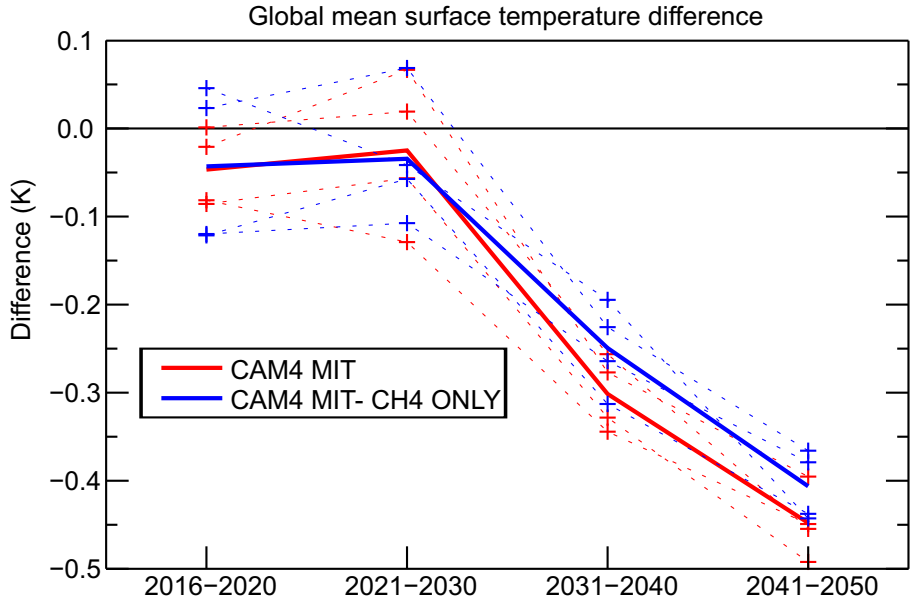

Figure 18. Time evolution of differences in global mean surface temperature between transient simulations following the mitigation (MIT) and the current legislation (CLE) scenario (i.e., MIT-CLE), as simulated by the CESM-CAM4 model with a slab-ocean representation. One experiment (red lines) included all emission reductions of the MIT scenario, whereas another experiment (blue lines) included only the CH_4 emission reductions of the MIT scenario. Ensemble mean results are shown with thick lines, individual ensemble members with thin lines.

ACPD
15, 15155–15241, 2015

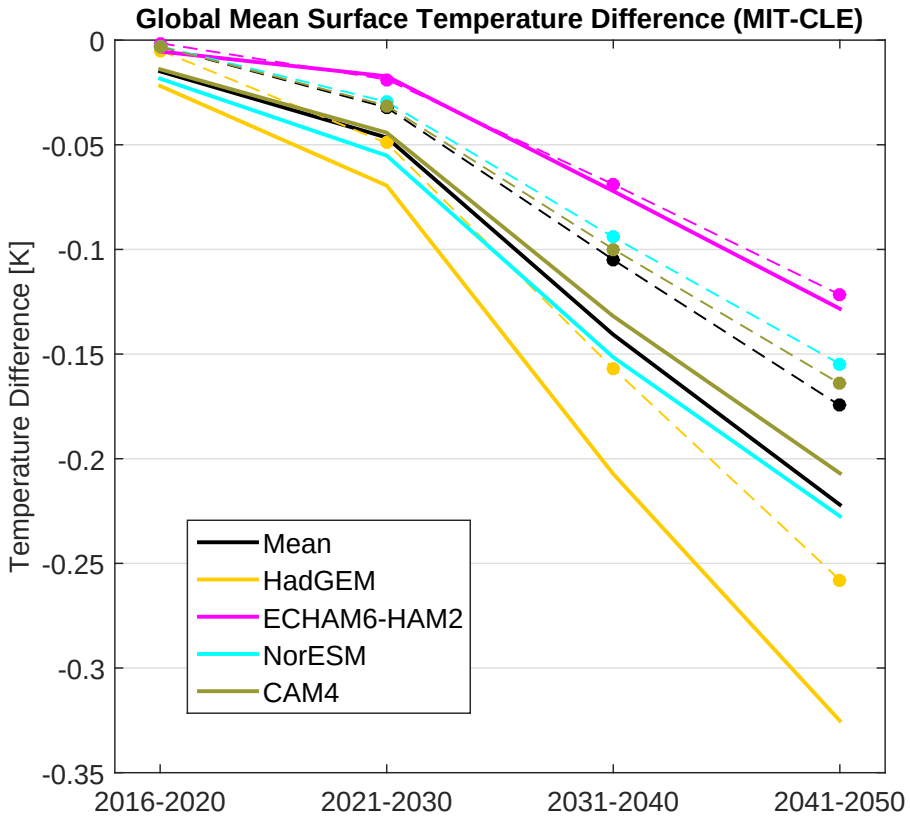

Figure 19. Time evolution of difference in global mean surface temperature for the MIT and CLE scenario calculated with the ARTP-based method. Solid lines are the total difference (MIT-CLE), while the dashed lines give the responses to CH_4 mitigation only. The solid lines can be compared directly with the results from the transient model simulations shown in Fig. 14.

ACPD
15, 15155–15241, 2015

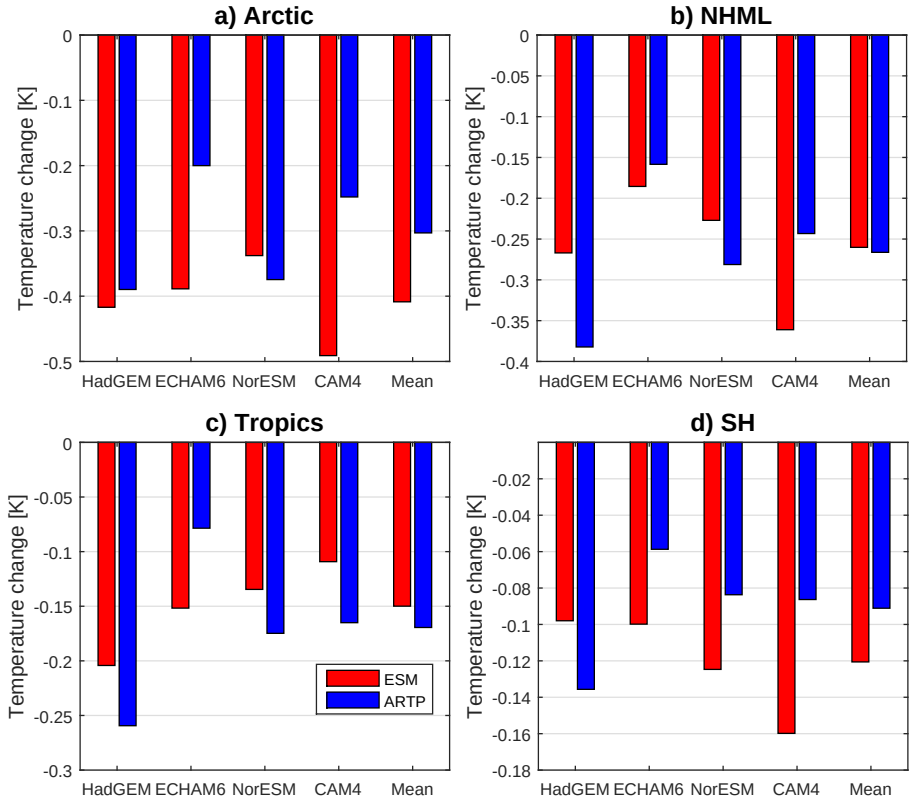

Figure 20. Temperature changes (MIT-CLE) in four latitude bands (Arctic, Northern Hemisphere Mid-Latitudes (NHML), Tropics and Southern Hemisphere) calculated with the ESMs and ARTP-based method. Mean changes over the 2031–2050 period are shown for individual models and the mean over the models. Notice the different temperature scales.

ACPD
15, 15155–15241, 2015

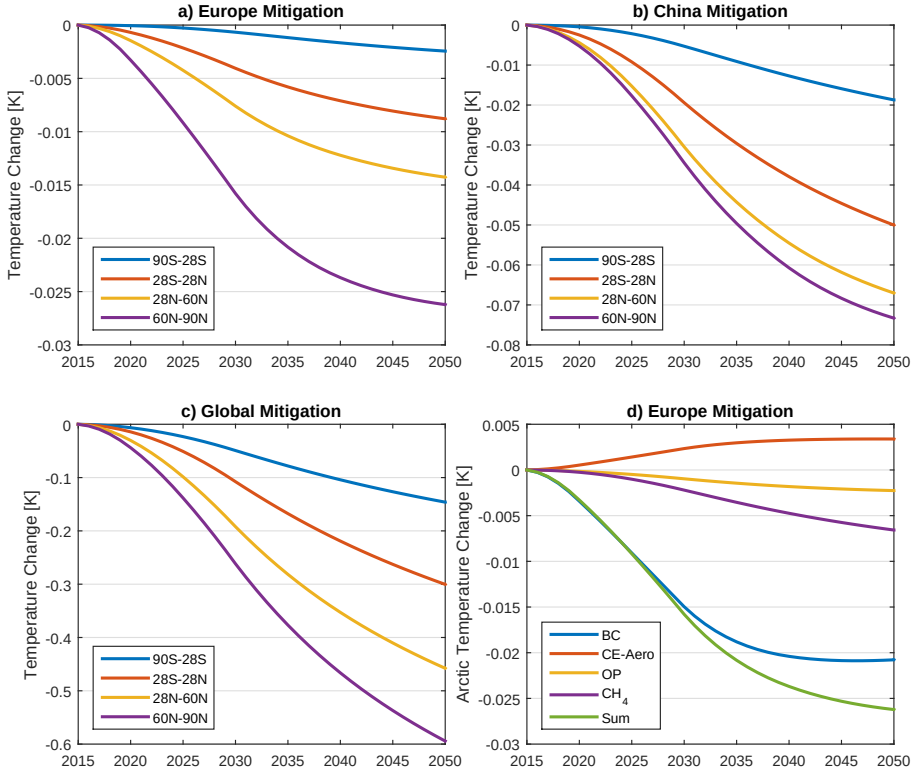

Figure 21. Annual mean surface temperature changes estimated by the ARTP method. **(a–c)** Changes in four latitude bands due to ECLIPSE mitigation scenario (MIT-CLE) for mitigation in Europe **(a)**, China **(b)** and globally **(c)**. **(d)** Arctic temperature changes due to mitigation of individual components from Europe. CE-Aero: Co-emitted aerosol (precursor) species (OA, SO_2 and NH_3), OP: Ozone precursors (NO_x, CO and NMVOCs). Note the different scales on the vertical axes.

ACPD
15, 15155–15241, 2015

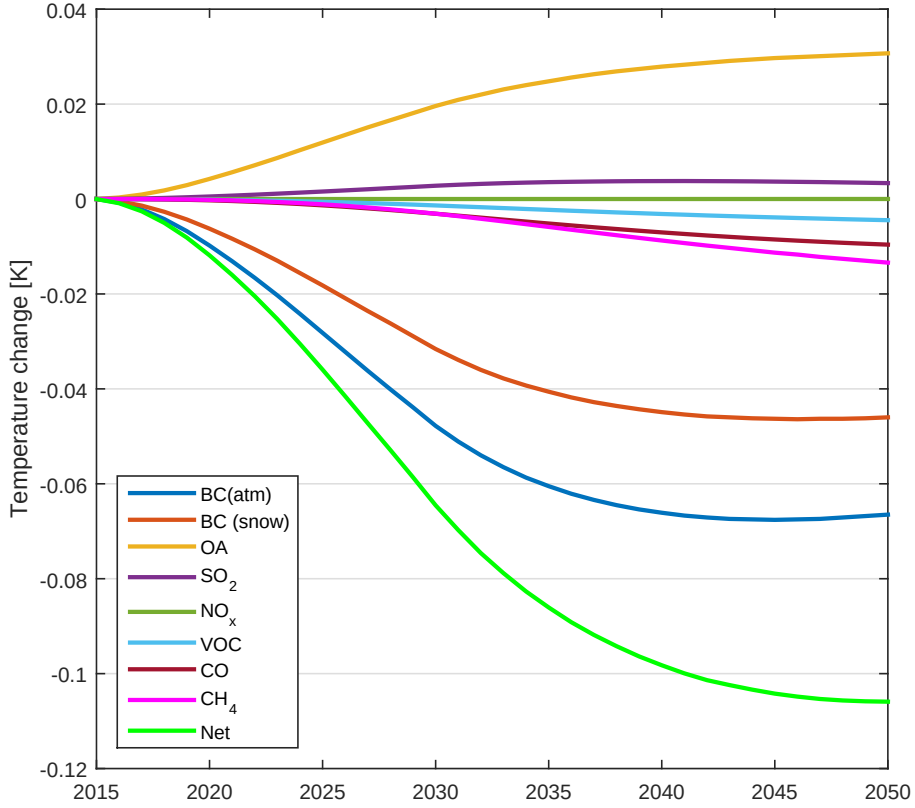

Figure 22. Total Arctic surface temperature change (K) by global mitigation of residential burning (heating and cooking) in the ECLIPSE emission scenario (MIT-CLE), as obtained with the ARTP method.

ACPD
15, 15155–15241, 2015